

Review article

Sugarcane health monitoring with satellite spectroscopy and machine learning: A review

Ethan Kane Waters*, Carla Chia-Ming Chen, Mostafa Rahimi Azghadi

College of Science and Engineering, James Cook University, 1 James Cook Dr, Douglas, Townsville, 4814, QLD, Australia

Agriculture Technology and Adoption Centre, James Cook University, 1 James Cook Dr, Douglas, Townsville, 4814, QLD, Australia



ARTICLE INFO

Keywords:

Sugarcane
Health monitoring system
Remote sensing
Satellites
Spectroscopy
Machine learning
Vegetation indices
Disease
Pests

ABSTRACT

Research into large-scale crop monitoring has flourished due to increased accessibility to satellite imagery. This review delves into previously unexplored and under-explored areas in sugarcane health monitoring and disease/pest detection using satellite-based spectroscopy and Machine Learning (ML). It discusses key considerations in system development, including relevant satellites, vegetation indices, ML methods, factors influencing sugarcane reflectance, optimal growth conditions, common diseases, and traditional detection methods. Many studies highlight how factors like crop age, soil type, viewing angle, water content, recent weather patterns, and sugarcane variety can impact spectral reflectance, affecting the accuracy of health assessments via spectroscopy. However, these variables have not been fully considered in the literature. In addition, the current literature lacks comprehensive comparisons between ML techniques and vegetation indices. This review addresses these gaps and discusses that, while current findings suggest the potential for an ML-driven satellite spectroscopy system for monitoring sugarcane health, further research is essential. This paper offers a comprehensive analysis of previous research to aid in unlocking this potential and advancing the development of an effective sugarcane health monitoring system using satellite technology.

Contents

1. Introduction	2
2. Literature search methodology	2
3. Sugarcane health conditions & growth limiting factors.....	3
3.1. Sugarcane diseases	3
3.2. Sugarcane pests.....	4
4. Spectral imagery.....	4
4.1. Large scale spectroscopy	5
4.1.1. Hyperspectral.....	5
4.1.2. Multispectral.....	5
4.2. Small scale spectroscopy	6
5. Satellites for vegetation health monitoring.....	6
5.1. Satellite selection considerations.....	6
5.2. Satellite limitations.....	7
6. Vegetation indices.....	8
7. Influential factors on sugarcane reflectance.....	9
7.1. Sugarcane variety	9
7.2. Meteorological effects	9
7.3. Temporal morphological changes & multi-temporal analysis.....	11
7.4. Viewing angle of vegetation	12
8. Machine learning algorithms and methods of analysis.....	12
9. Conclusion and future work.....	13
CRediT authorship contribution statement	14

* Correspondence to: 1 James Cook Dr, Douglas, Townsville, QLD 4814, Australia.

E-mail addresses: ethan.waters@jcu.edu.au (E.K. Waters), carla.ewels@jcu.edu.au (C.C.-M. Chen), mostafa.rahimiazghadi@jcu.edu.au (M. Rahimi Azghadi).

Declaration of Generative AI and AI-assisted technologies in the writing process	14
Declaration of competing interest.....	14
Data availability	14
References.....	14

1. Introduction

The Earth's population has rapidly increased from 2.5 billion in 1950 to over 8 billion in 2024. This change has reflected a significant increase in the aggregate agricultural production to sustain the population (Nikos Alexandratos, 2012; Zabel et al., 2014; Magarey, 2021). The global population growth is projected to reach 9.15 billion by 2050 and is expected to require a 70% increase in aggregate agricultural production from 2012 (Nikos Alexandratos, 2012; Zabel et al., 2014; Tilman et al., 2011; Godfray et al., 2010; Gregory and George, 2011). Improving yield and agricultural production through traditional methods has become increasingly challenging, leading to a growing demand for smart agricultural practices. (Nikos Alexandratos, 2012). Sugarcane is one of the world's most important agricultural products, which is grown and produced in large volumes. For instance, it was reported that in 2021, global sugarcane production was 1861.9 billion kilograms. Australia produced 31.13 billion kilograms in 2021 (Food and Agriculture Organization of the United Nations, 2023), putting it ninth for worldwide production, where 95% of production occurred in the state of Queensland. Sugarcane yield can be heavily hampered by the impact of a variety of health conditions. Diseases such as Ratoon Stunting Disease (RSD), Orange Rust, and Sugarcane Yellow Leaf Virus (SCYLV) can reduce yield by between 43% and 50% in severe circumstances (Rassaby et al., 2003; Magarey et al., 2004; Ramouthar et al., 2013; Bailey and Bechet, 1986). A study by Magarey et al. (2021), suggested that in 2019, there was an annual economic loss of \$25 million as a result of RSD infection with varying rates of incident across 87000 ha of sugarcane in Australia. Other factors that diminish crop health and contribute to a reduction in sugarcane yield include parasites, crop stress, and irrigation problems (for irrigated cane). Implementing methods to easily diagnose and early detection of any of these conditions on a large scale is vital for improving yield and the overall farming economics.

There are several methods the agricultural industry currently utilizes to determine existing health conditions. The key motivation behind these health monitoring technologies is to increase the likelihood of early detection, preventing the condition from spreading or further deterioration in currently affected crops. A majority of current disease detection methods require visual inspection of symptoms or laboratory testing to conclusively determine the presence of a disease (Zhu et al., 2010; Carvalho et al., 2016; Young et al., 2016; Fegan et al., 1998; Ghai et al., 2014). Although accurate, collecting and testing enough samples to adequately evaluate the health of the crops is time-consuming and infeasible in large-scale agriculture. For example, the average sugarcane farm in Queensland is 110 Ha as of 2019 (Canegrowers, 2019) which makes visual inspection and sample collection challenging. Many sugarcane diseases can be identified by the morphological changes they cause. However, some diseases are asymptomatic and consequently, visual inspection may not be reliable for disease identification (Grisham et al., 2010). Furthermore, sugarcane can grow to a height of 2 to 7 meters and form very dense vegetation, making it difficult for personnel to traverse mature fields and consequently, perform visual inspections of mature crops (Som-ard et al., 2021; Yamane, 2019). Thus, it would be beneficial to implement large-scale remote sensing for crop health monitoring that could identify crop health hazards before widespread impact and/or visible symptoms.

Several studies have shown the possibility of distinguishing healthy and unhealthy sugarcane without traditional laboratory testing (Apan et al., 2004; Moriya et al., 2017; Grisham et al., 2010; Narmilan et al.,

2022; Simões and Rios do Amaral, 2023; Ong et al., 2023; Johansen et al., 2014, 2018; Vargas et al., 2016). These studies focused on determining if there is a distinctive difference in the spectral reflectance of healthy and unhealthy crops with field spectroscopy for a variety of diseases. There was a 73% and 96.2% accuracy in identifying SCYLV and Orange Rust disease in sugarcane with hyperspectral imaging (Grisham et al., 2010; Apan et al., 2004, 2003). In addition to sugarcane, multispectral imaging has been seen to be an effective disease detection method in other crops, with an 88% accuracy in detecting several diseases in wheat, which like sugarcane is a perennial grass (Franke and Menz, 2007). Spectroscopy provides an opportunity to be able to diagnose health conditions at the plantations, which may not be visible to the human eye. Alternatively, true colour RGB images remain a viable option for disease and pest detection with neural networks or ML algorithms, especially when visible symptoms are present (Militeanu et al., 2019; Srivastava et al., 2020; Ratnasari et al., 2014). However, a key limitation of RGB imaging is that asymptomatic conditions or subtle symptoms can easily go undetected, making it less reliable in cases where early or non-visible symptoms of a disease are critical for its diagnosis.

Vegetation monitoring extends beyond the scope of vegetation health monitoring, encompassing a broader set of tasks such as yield prediction, and fertilizer optimization. These additional areas of study have seen success with the application of ML and deep learning techniques to both true colour RGB and spectral images (Sanchez et al., 2018; Fernandes et al., 2017; Rahman and Robson, 2016; Everingham et al., 2016; Canata et al., 2021; Shendryk et al., 2020). However, these topics fall outside the scope of this review, as they have been extensively covered in other recent review papers (Garcia et al., 2022; de França e Silva et al., 2024).

This review aims to critically assess the current literature on health condition monitoring in sugarcane with ML algorithms that leverage satellite spectroscopy data. Additionally, we aim to collate, synthesize, and compare relevant literature on influential factors pertaining to the possible development of a large-scale health monitoring system for sugarcane with freely available satellite-based spectroscopy and ML. A summary of the collated research is shown in Table 1, with the inclusion of examples of two other crops that are relevant to the research objectives of this review.

Gaps in the literature regarding a system of this nature can then be identified and discussed with the overall objective of increasing the prevalence of satellite-sensing-based precision agriculture in the sugarcane industry to increase yield. Influential factors identified and discussed include:

1. Relevant information regarding sugarcane disease, growth limiting factors, optimal growth conditions and traditional disease detection methods.
2. The most appropriate freely available satellites.
3. Relevant vegetation indices.
4. Factors that influence the observed reflectance of sugarcane.
5. Utilized ML methodology and approach.

2. Literature search methodology

Google Scholar returned 15 relevant papers published before January 2024 on the possible development of a sugarcane health monitoring system with satellite-based spectroscopy. The Keywords initially utilized to identify literature were "sugarcane", "disease", "remote

Table 1
Current multispectral and hyperspectral monitoring studies relevant to the development of a large scale sugarcane health monitoring system.

Reference	Health condition	Crop	Spectroscopy	Category	Satellite name	Time series	ML algorithm	Best classification accuracy
Apan et al. (2004, 2003)	Orange Rust	Sugarcane	Hyperspectral	Satellite	EO-1 Hyperion	False	LDA	96.90%
Moriya et al. (2017)	Mosaic	Sugarcane	Hyperspectral	Drone	N/A	False	SID	92.50%
Grisham et al. (2010)	SCYLV	Sugarcane	Hyperspectral	Handheld Spectrometer	N/A	True	LDA	73%
Narmilan et al. (2022)	White Leaf Disease	Sugarcane	Multispectral	Drone	N/A	False	RF, DT, KNN, XGB	92%, 91%, 92%, 92%
Simões and Rios do Amaral (2023)	Orange & Brown Rust	Sugarcane	Multispectral	Drone	N/A	False	RF, KNN, SVM	90%, 90%, 90%; 86%, 83%, 85%
Ong et al. (2023)	Brown Stripe & Ring Spot	Sugarcane	Hyperspectral	Handheld Spectrometer	N/A	False	RF, SVM, NB	95%, 88%, 77%
Franke and Menz (2007)	Powdery Mildew & leaf rust	Wheat	Multispectral	Satellite	QuickBird	True	DT	56.8%, 65.9%, 88.6%
Johansen et al. (2014)	Cane Grub	Sugarcane	Multispectral	Satellite	Geo-Eye1	False	GEOBIA	79%
Johansen et al. (2018)	Cane Grub	Sugarcane	Multispectral	Satellite	Geo-Eye1	False	GEOBIA	98.7%
Dutia et al. (2006)	Non-specific	Mustard	Hyperspectral & Multispectral	Satellite	EO-1 Hyperion & LISS-IV	False	DT	N/A
Bao et al. (2021)	Smut	Sugarcane	Hyperspectral	Handheld Spectrometer	N/A	False	CNN	>90%
Vargas et al. (2016)	Diatraea saccharalis	Sugarcane	Hyperspectral & Multispectral	Handheld Spectrometer & Satellite	Landsat 8	False	N/A	79.8% & 85.5%
Abdel-Rahman et al. (2010)	Thrips	Sugarcane	Hyperspectral	Handheld Spectrometer	N/A	True	N/A	N/A
Soca-Muñoz et al. (2020)	Orange & Brown Rust	Sugarcane	Hyperspectral & Multispectral	Handheld Spectrometer & Drone	N/A	False	N/A	N/A

sensing”, “pest”, “health monitoring”, “spectroscopy”, “vegetation index”, “reflectance” and “satellite”. This search only evaluated literature to be relevant if it contained at least five of the nine specified keywords. Our literature search methodology is reported in Fig. 1. Through this review process, key factors relevant to the development of this system were identified.

3. Sugarcane health conditions & growth limiting factors

3.1. Sugarcane diseases

Diseases pose a significant challenge in sugarcane cultivation, necessitating the development of more sophisticated detection methods to aid in management and increase yield. Orange rust is a disease caused by the pathogen *Puccinia kuehni* which produces orange patchy lesions (Magarey et al., 2022). Infection typically occurs in wet humid conditions and is propagated by water, resulting in yield losses of up to 38% (Magarey et al., 2004). *Puccinia melanocephala* is the causal agent for Brown rust which bears resemblance to orange rust with the variation between them suggested in their names. Yield losses of up to 22% have been observed as a result of brown rust infection which typically occurs in dryer climates. Similar to the preceding health conditions, the Sugarcane Mosaic Virus which is a *Potyvirus* has visible symptoms present on the foliage. Transmission of Sugarcane Mosaic Virus in nature is primarily several aphid vectors (Lu et al., 2021) such as *Hysteroneura setariae* (Lu et al., 2021), *Longiunguis sacchari* (Singh et al., 2005), *Rhopalosiphum maidis* (Brandes et al., 1920), and *Toxoptera graminum* (Lu et al., 2021). Once infected, the virus can reduce yield by 10% to 50% depending on the susceptibility of the variety and its

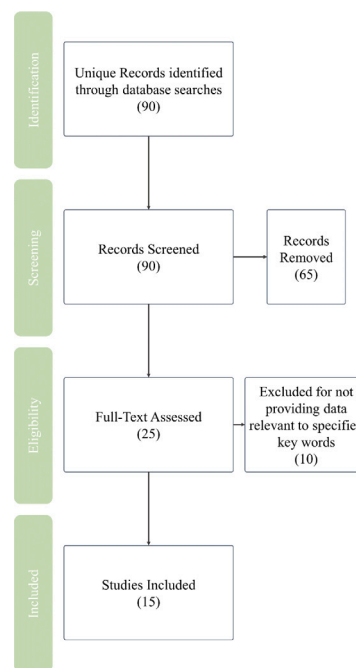


Fig. 1. Literature Review flow diagram.

region of origin (Singh et al., 2003; Matsuoka and Maccheroni, 2015; Singh et al., 1997; Koike and Gillaspie, 1989). Although these diseases can cause significant yield loss, a large number of current commercial sugarcane varieties in Australia are resistant to Orange rust, Brown rust and Mosaic virus (SRA, 2022). Significant losses of at least 50% have been previously observed (Agnihotri, 1983) as a result of White Leaf disease. This disease is caused by *phytoplasma* and can be visually identified from the striking white foliage. Wang et al. (2021) observed that Brown Stripe can result in yield losses of up to 40% (Magarey et al., 2022). Brown Stripe is often in the presence of poor soil nutrition and is propagated by a fungus *Bipolaris stenospila*. SCYLV has been observed to cause up to 37% yield loss Rassaby et al. (2003). Despite visual discolouration, Ring spot causes no reduction in yield and has no recommended treatment as a result (Magarey et al., 2022). The resistance of Australian sugarcane varieties to Ring Spot, Brown Stripe, White Lead Disease and SCYLV are not known (SRA, 2022).

Unlike the preceding conditions, some sugarcane diseases such as RSD do not typically exhibit easily identifiable symptoms (Magarey, 2021; Magarey et al., 2022). RSD is caused by a bacteria, *Leifsonia xyli*, which infects the xylem vessels of the sugarcane (Magarey, 2021; Davis et al., 1984). It has been indicated that sugarcane in some regions is significantly more susceptible to RSD than other known diseases (SRA, 2022). In order to officially diagnose RSD, one of the following tests must be performed; evaporative-binding enzyme-linked immunoassay (EB-ELISA) or polymerase chain reaction (PCR). These tests are time- and cost-prohibitive, and are difficult to perform on large scales (Zhu et al., 2010; Magarey, 2021). The development of a large-scale continuous monitoring and detection method would, therefore, increase the detection of disease, helping to prevent further spread.

A practical solution to a large-scale sugarcane health monitoring system will need to be capable of identifying health conditions simultaneously. However, currently, only one study has attempted to classify multiple conditions (Ong et al., 2023). Spectroscopy has been most commonly utilized in studies that consider Orange Rust and Brown Rust (Soca-Muñoz et al., 2020; Apan et al., 2004, 2003; Simões and Rios do Amaral, 2023). This is done even though a majority of commercially used varieties are sufficiently resistant to the disease (SRA, 2022). It was observed that the greatest variation in the electromagnetic spectrum for both diseases occurred in the visible and NIR regions (Soca-Muñoz et al., 2020; Apan et al., 2004, 2003). These studies utilized either hyperspectral or multispectral imaging, and at different scales with a combination of Satellites, drones and handheld spectrometers employed. Where ML was implemented, orange rust was more accurately detected than any other disease with classification accuracies between 90% and 96.9%.

While Orange Rust has been more accurately classified in the existing literature, there are certain factors inherent in the methodology of this classification that potentially contribute to this trend. Although the study by Simões and Rios do Amaral (2023) maintained a consistent methodology, it primarily focused on classifying varieties resistant to Orange and Brown rust, rather than identifying infected vegetation. Consequently, additional research is necessary to ascertain which regions of the electromagnetic spectrum exhibit the most significant variation due to specific symptoms and to validate that the specified diseases can be reliably distinguished from healthy sugarcane.

3.2. Sugarcane pests

Similar to diseases, pests also contribute to a severe reduction in sugarcane yields worldwide. A prominent pest in Central and South America is a species of moth, *Diatraea saccharalis*, whose larvae bore into the internodes resulting in a yield reduction of between 13.5% and 21.0% (de S. Rossato, Jr. et al., 2013). This is similar to the 13% yield reduction observed across the industry between 1935 and 1957 by Hensley (1971) and in recent years a simple conservative estimation of yield loss was generalized to 0.77% per 1% of damaged

internodes (Macedo et al., 2015). Thrips (*Thysanoptera*) pose a similar threat to sugarcane in Southeast Asia, South Africa and Australia by eating the sugarcane leaves, causing lacerations and discolouration resulting in yield reductions of between 18.0% and 26.8% (Way et al., 2006, 2010).

Contrary to the aforementioned pests, Canegrubs (*Melolonthinae* larvae) feed on the root system of sugarcane which results in reduced growth, lodging or plant death, significantly affecting the sugarcane industry. For instance, this pest could cost the Australian sugarcane industry an estimated \$40 million during severe outbreaks (Sallam, 2011; Keith, 2002).

The field of sugarcane pest detection has seen significant advancements, with various studies employing diverse methodologies and technologies. Notably, Canegrub infestations have been a focal point of research with recent studies (Johansen et al., 2014, 2018) investigating the infestations with multispectral imagery from the Geo-Eye1 satellite, employing Geographic Object-Based Image Analysis (GEOBIA) achieving classification accuracies of between 75% and 98.7%. Unlike diseases that may exhibit spectral variations related to moisture content, the symptoms of Canegrub infestations, often leading to lodging and significant soil exposure, influence the visible and near-infrared (NIR) spectra more significantly. Consequently, the detection of Canegrub infestations appears to be less dependent on water absorption bands and may contribute to the high classification accuracy of Canegrub symptoms whilst being constrained to wavelengths smaller than 1000 nm.

Vargas et al. (2016) focused on *Diatraea saccharalis*, utilizing hyperspectral and multispectral data from Landsat 8 and a handheld spectrometer. Their approach, achieving classification accuracies of 79.8% and 85.5%, highlights the significance of incorporating various sensing technologies. However, the methodology and the explanation lack clarity. In contrast, Abdel-Rahman et al. (2010) explored Thrips detection using hyperspectral data and a handheld spectrometer. While specific accuracy metrics are not provided, the study emphasizes the potential of hyperspectral imaging for pest identification.

Despite advancements, the field faces challenges similar to those in disease detection, including a lack of standardization and consistency among studies. Further research is warranted to identify optimal spectral regions for discerning specific pest-induced symptoms and to enhance the reliability of pest detection methodologies in sugarcane cultivation. Additionally, the development of a large-scale continuous monitoring and detection method would increase the detection of these pests, providing the opportunity to implement targeted control measures. Therefore, in this study, we focus on the conditions that have been detected using satellite-based spectroscopy where possible, in particular hyperspectral and multispectral images.

4. Spectral imagery

Hyperspectral and multispectral imaging are two forms of spectroscopy, which measure the reflected electromagnetic radiation from an object. These measurements capture several “bands” across the electromagnetic spectrum, encompassing both visible and non-visible light (Storch, 2022; Goetz et al., 1985). A band is described as a small section of the electromagnetic spectrum. Each image captured is three-dimensional, consisting of an x and y spatial dimension, and a spectral dimension. The spatial resolution is defined by the physical dimensions of each pixel, while the spectral resolution is characterized by the number and size of the bands captured. Hyperspectral imaging involves capturing a continuous set of narrow bands within the range of 400 nm to 2500 nm, typically with intervals less than 10 nm (Storch, 2022; Goetz et al., 1985; Sahoo et al., 2015). This allows for the formation of high-resolution continuous spectral signatures. In contrast, multispectral imaging captures the spectral information for a discrete number of bands within the same range, generally with bandwidths

between 20 and 200 nm (ElMasry and Sun, 2010). Consequently, multi-spectral imaging has much lower spectral resolution than hyperspectral imaging. Although higher spectral resolution is desirable, it comes with increased complexity and computational requirements. Additionally, there are significantly fewer satellites available with hyperspectral imaging capabilities than multispectral imaging. It is important to note that both hyperspectral and multispectral imaging can be captured at different spatial scales. Small-scale observations are often acquired using drones or handheld spectrometers, while large-scale assessments are conducted through satellite platforms. This variation in spatial scales introduces important considerations when interpreting and comparing findings in precision agriculture and remote sensing. The choice of sensor platform greatly influences the spectral and spatial resolution of the captured image. To overcome limitations in either spatial or spectral resolution, image fusion techniques can be employed, to combine high spatial resolution panchromatic images with low spatial resolution spectroscopy data (Sara et al., 2021a; Yilmaz and Gungor, 2016). This approach enhances image quality and can overcome potential limitations of scale or resolution associated with drones or satellites.

Typically in studies that demonstrated lower rates of classification, the spectral reflectance measurements were limited to 1000 nm or less (Grisham et al., 2010; Franke and Menz, 2007; Johansen et al., 2014; Vargas et al., 2016). In contrast, sensors with a wider spectral range typically exhibited higher classification rates (Simões and Rios do Amaral, 2023; Ong et al., 2023; Apan et al., 2003). This is not a strict rule given that high classification rates were still seen with a limited spectral range (Moriya et al., 2017; Narmilan et al., 2022). However, it is essential to note that the observed high rates of classification in these studies may be attributed to the specific characteristics of the diseases investigated. For instance, the diseases examined in these studies are known to cause white or significantly light discoloration in the leaves. The distinctive changes in the visible region of the electromagnetic spectrum could have been pronounced enough to achieve accurate classification without the need for additional information, thereby reducing the reliance on information from wavelengths beyond 1000 nm. While studies focusing on diseases with different visual symptoms may necessitate a broader spectral range for effective classification, the particularities of the diseases considered in the cited research may explain success with limited spectral measurements.

An alternative satellite-based sensor to spectroscopy for vegetation health monitoring is Synthetic Aperture Radar (SAR). Although SAR primarily provides data about surface structure and topology, it has proven effective in applications such as sugarcane growth monitoring and plantation mapping (Hong et al., 2024; Baghdadi et al., 2009; Li et al., 2019; Wang et al., 2020). One of SAR's key advantages is its ability to operate independently of cloud cover, making it highly reliable for continuous monitoring in areas with frequent cloud interference. For an in-depth review of SAR's application in vegetation health monitoring, readers can refer to the relevant literature (McNairn and Shang, 2016), as this topic falls beyond the scope of this review.

4.1. Large scale spectroscopy

4.1.1. Hyperspectral

The only study to date which classifies diseased sugarcane with satellite-based hyperspectral imaging was conducted by Apan et al. (2003). The study effectively addresses noise and atmospheric effects through standard techniques of its time. This demonstrates potential for automation in developing an efficient health monitoring system after updating to more recent techniques and scaling the approach. The study found distinct spectral reflectance variations between healthy and unhealthy sugarcane across the electromagnetic spectrum. The high spectral resolution of hyperspectral imagery offers the advantage of capturing nuanced differences specific to particular health conditions, which may make it preferable when developing sophisticated models that differentiate multiple conditions. However, limitations due to data

storage and processing power at the specified satellite sampling frequency may necessitate compromising accuracy. Multispectral imaging may be an effective compromise for these constraints, but further research is required to adequately conclude the required or ideal spectral resolution for large scale sugarcane health monitoring systems. Furthermore, additional investigations are essential to ascertain the reproducibility of these findings for various health conditions, sugarcane varieties, across diverse regions and under varying meteorological conditions preceding the acquisition of satellite imagery. The implications of these investigations significantly influence the feasibility of establishing a robust health monitoring system that is financially viable.

4.1.2. Multispectral

Sugarcane health condition monitoring with satellite-based multispectral imaging has seen more attention than its hyperspectral counterpart (Vargas et al., 2016; Johansen et al., 2014, 2018). These studies all focus on pests and there are currently no studies that demonstrate the efficacy of satellite-based multispectral imaging for discerning various sugarcane diseases. Consequently, there is a lack of assessments against hyperspectral imagery counterparts with established disease detection methods. Additionally, the optimal number of bands and their respective bandwidths for multispectral satellites has yet to be determined in the context of differentiating sugarcane health conditions. Although Galvão et al. (2006) compared the effect of bandwidth, they predominantly utilized satellites that are no longer in operation. Therefore, there is a prevailing need to revisit and refine this investigation using contemporary satellites.

The health condition monitoring study by Johansen et al. (2014), mapped canegrub damage using satellite-based multispectral imaging and achieved classification accuracies of between 53%–79%. They further improved the accuracy of canegrub damage detection to between 75% and 98.7% through the implementation of a spectral difference segmentation algorithm into their established method (Johansen et al., 2018). Both models implemented a Geographic Object-Based Image Analysis (GEOBIA) approach to consider contextual and shape information in the analysis. Both studies derived the NDVI to indicate vegetation health and assessed the standard deviation of the red spectral band to indicate the texture. Empirically derived thresholds were established for the 30-quantile of NDVI and the 70-quantile of the red spectral band standard deviation. Regions falling below the 30-quantile and surpassing the 70-quantile were identified as potential areas affected by canegrub damage. The severity of the damage was classified using a set of undisclosed thresholds based on the relative differences in NDVI and texture values compared to the rest of the block, however, the rationale behind determining these thresholds was not included in the paper. Additionally, there was little information on the effectiveness of the models' ability to distinguish between canegrub damage and analogous symptoms such as lodging.

Duft et al. (2019) performed sugarcane variety classification in Brazil using Sentinel-2 image and found that multispectral satellites can be utilized to perform classification of sugarcane based on variations in spectral reflectance. Although there are only a few studies on using satellite-based multispectral imaging in sugarcane health monitoring, it has been used in several studies monitoring the health of other crops. For example, the study by Dutia et al. (2006) incorporated multispectral imaging from LISS-IV in image fusion where images of high spectral resolution are fused with images of high spatial resolution to estimate an image of both high spatial and spectral resolution (Sara et al., 2021b; Feng et al., 2020). However, the complexity of this approach hinders a direct assessment of the sustainability of satellite-based multispectral imagery for a large-scale health monitoring system for sugarcane. Consequently, the lack of clarity on the minimum required spatial resolution for effective health monitoring and the potential impact of atmospheric conditions on the viability of satellite-based imagery for this purpose underscores the need for further studies in this domain. Once a comprehensive understanding of the impacts associated with

the choice of sensor, in the context of sugarcane health monitoring, is established, the implementation of image fusion should be explored further. The ability to combine the strengths of high-spectral-resolution and high-spatial-resolution images, positions image fusion as a powerful technique with the potential to enhance the overall effectiveness of monitoring systems. This approach, when employed effectively, can contribute to more accurate and detailed insights into sugarcane health, paving the way for advanced disease detection methodologies, once the fundamentals have been sufficiently understood.

In another example of using multispectral satellite for health monitoring, Franke and Menz (2007) found multispectral imaging could be utilized to detect powdery mildew and leaf rust in wheat. This indicates it may be plausible to adopt a similar approach in attempting to identify sugarcane-based health conditions with satellite-based multispectral imaging. However, the viability of a multispectral satellite for disease detection will vary for each satellite as each sensor will capture different bands with varying bandwidths and resolutions. Franke and Menz (2007) utilized the commercial high-resolution multispectral satellite QuickBird with a resolution of 2.4 m (European Space Agency, 2022c) and therefore a similar approach with a lower resolution freely available satellite for sugarcane may not yield as effective classification. Therefore, before attempting to determine the optimal characteristics of multispectral satellites for disease detection, the viability of conducting disease detection for sugarcane at all with the currently available free multispectral satellites should be investigated. The methodology required to perform disease detection with satellite-based multispectral imagery will remain consistent with the methodology to perform satellite-based hyperspectral disease detection, with variations in the vegetation indices and pre-processing methods utilized.

4.2. Small scale spectroscopy

The majority of previous studies for sugarcane were performed with field spectroscopy or drone rather than satellite (Moriya et al., 2017; Grisham et al., 2010; Narmilan et al., 2022; Simões and Rios do Amaral, 2023; Ong et al., 2023; Abdel-Rahman et al., 2010; Soca-Muñoz et al., 2020). The impracticality of field spectroscopy in sugarcane plantations stems from the crop's extensive scale and dense vegetation, rendering the approach comparable to traditional sampling methods without significant gains in detection capabilities. This comparison is valid, as a considerable number of diseases affecting sugarcane can be reliably diagnosed through visible inspections conducted by trained personnel (Julien et al., 1989; Magarey et al., 2022). While employing field spectroscopy may enhance confidence in diagnosis, it does not enhance the efficacy of performing widespread disease detection any more than employing trained field agronomists. The heart of the issue is that only sugarcane on the periphery of sugarcane plantations can be visually inspected. By the time the disease had spread to the visual periphery of the plantations, it would have likely become a widespread issue.

The majority of previous studies on sugarcane disease detection conducted in the last 5 years have favoured the use of drones (Moriya et al., 2017; Narmilan et al., 2022; Simões and Rios do Amaral, 2023; Soca-Muñoz et al., 2020). This trend suggests a shift towards approaches that offer more flexibility in terms of accessibility and manoeuvrability. The agility of disease detection tools is paramount for effective monitoring in the dynamic and expansive context of sugarcane plantations. Although drones can perform these tasks on a wider scale when compared with hand-held devices, typically drones are not capable of operating over distances as large as the standard sugarcane plantation and may require several flights. Furthermore, there are often stringent legal requirements for operating drones and costs associated with the acquisition of the drone. With that being said, it is essential to note that recent literature employing drones reported high classification results or statistically significant differences between healthy and diseased crops (Moriya et al., 2017; Simões and Rios do Amaral, 2023;

Narmilan et al., 2022; Soca-Muñoz et al., 2020). This is not unexpected considering the potential access to high spatial and spectral resolution spectroscopy when utilizing drones. Satellite-based remote sensing may provide an effective alternative or complementary solution for crop health monitoring at a sufficiently large scale, provided it is able to produce consistent comparable classification results as drone-based monitoring. Future studies should investigate trade-offs in classification accuracy and the logistics of each method for specific applications.

5. Satellites for vegetation health monitoring

Satellites have many applications in remote sensing, including but not limited to land surveying, earth science, and agriculture (Xue and Su, 2017; Guzmán Q. et al., 2023; Pandey et al., 2023; Emick et al., 2023). It is highly advantageous to use satellite-based remote sensing for large or inaccessible areas, where data collection would be infeasible using conventional methods. Satellite-based remote sensing varies depending on the sensor. Typically in agricultural applications sensors include radiometers, spectrometers, panchromatic cameras, and thermal imaging cameras. There are many commercial and freely available satellites with a combination of the aforementioned sensors. Commercial satellites are often costly, which makes them unsuitable for small farms or wide use. To facilitate satellite use for affordable monitoring applications, in this study, we only focus on freely available satellites. A list of these satellites appropriate for precision agriculture can be seen in Table 2.

5.1. Satellite selection considerations

An important factor to consider is the temporal resolution of a satellite, specifically the period of time taken to return to the same position at nadir, repeating cycles and revisiting times. A repeat cycle is the time it takes for the satellite to be centred at the same previous latitude and longitude coordinates, at the same angle. Whereas the revisit time is the period of time before the same location is surveyed again at all. This resolution has been increased by some satellites through the deployment of two identical satellites 180 degrees out of phase. This is the case for the series of satellites Sentinel-2 and Sentinel-3 or Landsat 8 and Landsat 9.

Another major factor to consider when selecting an appropriate satellite for precision agriculture is the spatial resolution. This varies significantly between satellites and is often significantly better for commercial satellites. There is often a trade off between high spatial and spectral resolution, consequently, several freely available multispectral satellites offer varying spatial resolutions depending on the spectral bands available. Therefore, it is important to ensure satellites with the desired spectral bands are available in the required spatial resolution as the variation can be significant. For example, Fig. 2 shows a visual comparison of a true colour image in the available Sentinel-2 spatial resolutions of 10 m, 20 m, and 60 m. Sentinel-2 captures data across 13 different spectral bands between approximately 400 nm and 2300 nm, however only the red, green, and blue spectral bands are available at every resolution (European Space Agency, 2022d; Slagter et al., 2023). There is only a single NIR band (Band 8) available with a 10 m spatial resolution, centred at 842 nm, in contrast to the four available in NIR region and two in the SWIR region at a spatial resolution of 20 m (European Space Agency, 2022d). Therefore, monitoring specific wavelengths may limit the spatial resolution when considering financial constraints. The trade-offs between sensors make certain satellites more suitable for specific applications. For instance, when financial limitations restrict the choice to freely available satellites, Landsat's panchromatic imagery can be utilized to enhance spatial resolution through pan-sharpening, particularly when the available band resolutions are inadequate. Pan-sharpening with Landsat has been widely applied in various fields, including vegetation mapping of sugarcane (Johnson et al., 2014; Sudianto et al., 2023).

Table 2
Current easily accessible and freely available multispectral and hyperspectral satellites that are deemed appropriate for precision agriculture.

Reference	Name	Sensor	Bands	Bandwidth (nm)	Wavelength range (nm)	Spatial resolution (m)	Partner satellite	Repeat cycle single satellite (Days)	Repeat cycle multiple satellite (Days)	Swath width (km)	Active
European Space Agency (2022d)	Sentinel-2A	Multispectral	13	Varies	420 – 2370	10, 20, 60	Sentinel-2B	10	5	290	23-06-15 to Present
European Space Agency (2022d)	Sentinel-2B	Multispectral	13	Varies	420 – 2370	10, 20, 60	Sentinel-2A	10	5	290	07-03-17 to Present
NASA (2022c)	Landsat 9	Multispectral, Panchromatic & Thermal	11	Varies		30, 15, 100	Landsat 8	16	8	185	27-9-21 to Present
NASA (2022b)	Landsat 8	Multispectral, Panchromatic & Thermal	11	Varies		30, 15, 100	Landsat 7, Landsat 9	16	8	185	11-02-20 to Present
NASA (2022a)	Landsat 7	Multispectral, Panchromatic & Thermal	8	Varies	450 – 2350	30, 15, 60	Landsat 8	16	8	185	15-04-99 to 27-09-21
SIIS (2010)	KOMPSAT-3	Multispectral & Panchromatic	5	Varies	450 – 900	2.0 , 0.5	N/a	28	N/A	16	17-05-12 to Present
SIIS (2010)	KOMPSAT-3A	Multispectral & Panchromatic	5	Varies	450 – 900	1.6 , 0.4	N/a	28	N/A	13	25-03-15 to Present
European Space Agency (2022b)	Proba-1 (CHRIS)	Hyperspectral	–	10	400 – 1300	17	N/a	7	N/A	14	22-10-01 to 4-05-21
European Space Agency (2022e)	SPOT-6	Multispectral & Panchromatic	5	Varies	450 – 890	6, 1.5	SPOT-7	26	13	60	30-06-14 to Present
European Space Agency (2022e)	SPOT-7	Multispectral & Panchromatic	5	Varies	450 – 890	6, 1.5	SPOT-6	26	13	60	30-06-14 to Present
European Space Agency (2022a)	EO1 Hyperion	Hyperspectral	–	10	357 – 2576	30	N/a	16	N/A	7.5	21-11-01 to 30-03-17
Galeazzi et al. (2008)	PRISMA	Hyperspectral	–	12	400 – 2500	30	N/a	29	N/A	30	22-03-19 to Present
Storch (2022)	EnMAP	Hyperspectral	–	6.5, 10	420 – 2450	30	N/a	27	N/A	30	01-04-22 to Present

5.2. Satellite limitations

Although satellites provide the ability for large-scale sensing, there are several limitations. Satellite imagery is susceptible to atmospheric effects, such as scattering or absorption, and require atmospheric correction to be applied to convert atmospheric radiance received by the satellite to an accurate surface reflection (Liang and Wang, 2020; Agapiou et al., 2011). The surface or “bottom-of-atmosphere” reflectance represents the true reflectance characteristics of the surface material. The atmospheric effects vary depending on the spectral band and were found to produce a mean difference of 18% between the NDVI of corrected and non-corrected values (Agapiou et al., 2011; Hadjimitsis et al., 2010). Several techniques and programs can be utilized to perform atmospheric correction.

A review of approaches to atmospheric correction was undertaken by Ientilucci and Adler-Golden (2019) which included several commercially available software packages. Quick Atmospheric Correction (QUAC) and Fast Line-of-Sight Atmospheric Analysis of Spectral Hypercubes (FLAASH) are two modules available for the software, Environment for Visualizing Images (ENVI), to perform atmospheric correction (Ientilucci and Adler-Golden, 2019; de los Reyes et al., 2020; L3Harris Software & Technology Inc, 2022). Other software such as Atmospheric and Topographic Correction (ATCOR) is available to perform atmospheric correction for a variety of remote sensing applications (Ientilucci and Adler-Golden, 2019; de los Reyes et al., 2020; ReSe, 2022). The Earth Resource Data Analysis System (ERDAS) and ENVI are software packages that can also perform a number of other remote sensing pre-processing tasks including destripping and image registration. The review conducted by Ientilucci and Adler-Golden (2019) highlighted that the performance of atmospheric correction techniques varied depending on the specific type of landscape in consideration. The Empirical Line Method (ELM) performed well (Ientilucci

and Adler-Golden, 2019), however it requires reflectance field measurements. Therefore, when evaluating atmospheric correction techniques for large-scale health monitoring, it is imperative to consider the landscape and logistical availability of spectrometers for quantitative calibrations. To complement these available tools, Quantum Geographic Information System (QGIS) is a widely adopted open-source GIS platform that provides the ability to visualize, edit and perform analyses with geospatial data (QGIS Development Team, 2024). While similar capabilities are available in commercial software, QGIS offers an extensive suite of tools that is freely accessible to the public, making it a valuable resource for a broad range of geospatial applications.

There are freely available packages capable of performing atmospheric correction. Python-Based Atmospheric Correction (PACO), is a Python library that is based on the ATCOR IDL code (de los Reyes et al., 2020). The initial release of the software is currently operational for Sentinel-2 series, Landsat –8, DESIS, and EnMAP satellites and currently has uncertainty values of approximately 30% and 10% for retrieval aerosol optical thickness and water vapour, respectively. Alternatively, Dark Object Subtraction (DOS) is a common and simple image-based technique that could be implemented for other satellites not supported by the PACO library (de los Reyes et al., 2020). This technique assumes that the pixels of the darkest object have a surface reflectance of approximately zero, and that the majority of the reflectance is a result of scattering in the visible light spectrum (Agapiou et al., 2011; Hadjimitsis et al., 2003). The average of the dark pixel values can be subtracted from all pixels in the image to adjust for the atmospheric affects. Satellites such as Sentinel-2 provide products with atmospheric correction pre-applied or the software to perform it.

Vegetation indices have been investigated and adapted as an alternative method to reduce the atmospheric effects. A new vegetation index, Atmospherically Resistant Vegetation Index (ARVI) was proposed to be utilized instead of NDVI with fewer atmospheric effects on

Sentinel-2 Spatial Resolution Comparison



Fig. 2. Spatial resolution comparison of available Sentinel-2 resolutions. Sentinel-2 offers four bands at 10 m resolution, ten bands at 20 m resolution and twelve bands at 60 m resolution.

the basis that the atmosphere significantly affects the red band (Xue and Su, 2017; Hadjimitsis et al., 2010; Agapiou et al., 2011).

6. Vegetation indices

Hyperspectral and multispectral imaging offer an alternative to traditional health monitoring by detecting changes in sugarcane spectral reflectance as a result of the health condition. These changes in spectral reflectance occur as a consequence of phenotypic and morphological changes incurred from the presence of disease or other conditions. A vegetation index is a transformation performed on the reflectance values measured with spectroscopy to evaluate the state of vegetation for a variety of applications in agriculture, environmental monitoring and ecosystem dynamics (Xue and Su, 2017). Vegetation indices aim to accentuate important characteristics of the vegetation and reduce the impact of redundant factors (Xue and Su, 2017; Fang and Liang, 2014). The result of the vegetation indices can then be utilized in algorithms to solve agriculture-related problems (Guzmán Q. et al., 2023; Xu et al., 2023). The applicability of a given vegetation index to an application is dependent on the sensor utilized to capture the spectral reflectance of the vegetation and the specific objective of the project (Xue and Su, 2017). Vegetation indices differ for hyperspectral and multispectral imaging as more specific bands with narrower bandwidths can be employed with hyperspectral imaging (Xue and Su, 2017).

A widely adopted and robust spectral vegetation index in precision agriculture and remote sensing is the Normalized Difference Vegetation Index (NDVI) (Xue and Su, 2017). It serves as a critical tool for assessing vegetation health, density, and productivity across various spatial and temporal scales. NDVI capitalizes on the spectral reflectance properties of plants, specifically their interaction with red and near-infrared (NIR) regions. Healthy vegetation strongly absorbs radiation in the red region for photosynthesis while reflecting a significant portion of NIR region due to leaf cellular structure (Xue and Su, 2017; Karnieli et al., 2010; Rouse et al., 1974). See for example, Fig. 3 which overlays an NDVI raster on a true colour image of sugarcane farms in the Herbert region of Queensland, Australia. This visually indicates variation between and within paddocks of sugarcane in the region, facilitating further investigation. NDVI and other commonly derived vegetation indices are widely accessible if users are unable to compute them directly. However, the resolution of these indices can vary significantly depending

on the source and associated costs. Pre-processed vegetation indices are available from a range of platforms, including NASA's Earthdata, the European Space Agency's Copernicus program, and commercial providers such as Planet Labs.

Apan et al. (2004, 2003) found success in developing five new vegetation indices, that consider the moisture content of vegetation and were dubbed the Disease-Water Stress Indices (DSWI). One of these indices was in the linear combination that achieved the highest overall accuracy of 96.9% for the classification of orange rust with LDA. Three out of the five DSWI had the highest canonical correlation with sugarcane infected with Orange Rust. The DSWI were formulated through the combination of Visible and Near-infrared (VNIR) and Short-Wave infrared (SWIR) reflectance bands which can indicate vegetation moisture content at wavelengths of 850, 1250, 1400 and 1650 nm (Gao, 1996; Apan et al., 2004; McFeeters, 1996; Hunt and Rock, 1989; Alves Varella et al., 2015). The effectiveness of DSWI for detecting orange rust is likely due to the patchy lesions caused by the fungal disease, which lead to moisture loss, changes in leaf structure, and plant stress. Therefore, it is reasonable to expect these indices to be effective for the detection of other diseases that alter the leaf structure or moisture content of vegetation (Dutia et al., 2006). The DSWI may not be effective for diseases that do not alter leaf structure, plant stress, and moisture content. For example, in the case of RSD, where the leaf structure of sugarcane remains the same and just the absorbance of water is affected (Magarey et al., 2022), the DSWI may not respond as effectively as a typical disease. This presents an opportunity to potentially utilize additional vegetation indices which focus on the moisture content of the vegetation (McFeeters, 1996; Hunt and Rock, 1989) or are combined with the DSWI (Xue and Su, 2017).

The prevailing trend in current literature predominantly focuses on the assessment of raw spectral measurements and at most a single individual vegetation index, with many studies neglecting to consider more than one (Grisham et al., 2010; Franke and Menz, 2007; Abdel-Rahman et al., 2010; Soca-Muñoz et al., 2020; Dutia et al., 2006; Vargas et al., 2016; Johansen et al., 2014, 2018; Moriya et al., 2017; Ong et al., 2023). This is despite the existence of several studies that assessed and showed that multiple vegetation indices consistently demonstrated high classification accuracies (Apan et al., 2003; Narmilan et al., 2022; Simões and Rios do Amaral, 2023). Previous success in classifying Orange Rust in sugarcane was found based on vegetation indices that

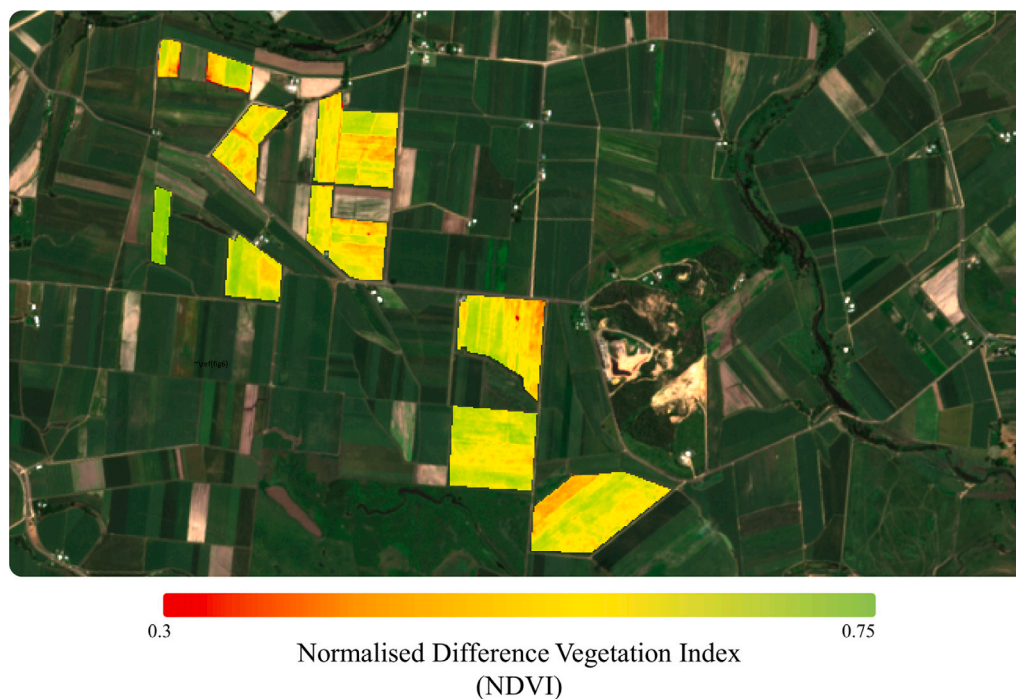


Fig. 3. Sentinel-2 10 m spatial resolution true colour image of sugarcane farms in the Herbert region of Queensland, Australia, overlaid with an NDVI raster.

accentuate variation in the moisture content of vegetation, thereby indicating that other moisture-based vegetation indices should be heavily considered in future studies. Table 3 contains vegetation indices from the collated literature which focus on changes in moisture content, leaf pigments, and leaf structure for plausible use in a sugarcane health monitoring system.

7. Influential factors on sugarcane reflectance

7.1. Sugarcane variety

The spectral reflectance of vegetation depends on the plant's physical and biochemical characteristics, including Leaf Area Index (LAI), leaf orientation, biomass, soil background, cell structure, moisture content and chlorophyll content (Alves Varella et al., 2015; Goetz et al., 1985; Sahoo et al., 2015; Roy and Ravan, 1996; Roy, 1989; Hapke, 1981; Hapke and Wells, 1981). Given that the varieties of sugarcane differ from one another, it is reasonable to expect their spectral reflectance would demonstrate a corresponding change. Galvão et al. (2006) found a significant difference in spectral reflectance of several Brazilian sugarcane varieties. Using multiple discriminant analysis (MDA), Galvão et al. (2006) were able to achieve 87.5% correct classification in identifying the variety (Galvão et al., 2005, 2006). Everingham et al. (2007) performed a similar study with varieties prominent in Australia during that time period, successfully discriminating sugarcane varieties with a number of ML techniques, among which random forest (RF) and support vector machine (SVM) were found to be the most effective with 87.5% and 90% per pixel classification accuracy. Both studies utilized the EO-1 Hyperion satellite and indicated that the spectral reflectance of different sugarcane varieties can vary substantially, with the regions of greatest separability seen in the Near Infrared (NIR) and Short-Wave Infrared (SWIR) regions (See Figure 2 in Everingham et al., 2007). Duft et al. (2019) corroborated these results by classifying varieties with a classification accuracy of 86% and 90% with Sentinel-2.

To establish an effective real-time disease and health monitoring system using satellite-based spectral imaging, it is essential to consider

variety as a crucial factor. Without accounting for variety-specific characteristics, the detection of variations in spectral reflectance due to health conditions across multiple sugarcane varieties becomes impractical. Despite these findings, only three health monitoring studies considered variety (Grisham et al., 2010; Moriya et al., 2017; Simões and Rios do Amaral, 2023). Unsurprisingly, Grisham et al. (2010) found that classification was more accurate when performed within a variety rather than across multiple varieties, as a consequence of spectral variation between varieties. It was demonstrated in Grisham et al. (2010) that SCYLV affects varieties differently with chlorophyll b levels of HO 95-988 remaining unaffected, but chlorophyll b levels of LCP 85-384 were significant when infected with SCYLV. This makes it reasonable to expect that sugarcane diseases may affect varieties in different manners and to different extents, incurring different alterations in the spectral reflectance. Similarly, it was demonstrated in a study conducted by Abdel-Rahman et al. (2010) that spectral reflectance of sugarcane varieties may react differently to Thrips damage. However, both studies conducted only featured two varieties of sugarcane and therefore further research should be conducted that considers variety as a factor.

7.2. Meteorological effects

The majority of research on large-scale sugarcane health monitoring was based on images at a single location at one point in time (Apan et al., 2004, 2003; Moriya et al., 2017; Narmilan et al., 2022; Johansen et al., 2014; Simões and Rios do Amaral, 2023; Abdel-Rahman et al., 2010). However, this prevailing pattern implies that annual variations in weather, such as temperature, humidity, sunlight duration, wind patterns and quantity of preceding rain, are not considered. By extension, it is currently unknown how effective a given method of health monitoring is when applied to different regions. Consequently, it is currently unknown whether the corresponding variation in these factors is considerable enough to impact the ability to discern health conditions with ML and therefore requires further research. Recognizing this limitation is imperative in the context of developing long-term

Table 3
Vegetation indices with a plausible application for sugarcane health monitoring.

Reference	Vegetation index	Formula
Rouse et al. (1974)	Normalized Difference Vegetation Index (NDVI)	$\frac{NIR-RED}{NIR+RED}$
Kaufman and Tanre (1992)	Atmospherically Resistant Vegetation Index (ARVI)	$\frac{NIR-(RED-BLUE)}{NIR+(RED-BLUE)}$
Genc et al. (2008)	Simple ratio index (SRI)	$\frac{NIR}{RED}$
Merzlyak et al. (1999c)	Plant Senescence Reflectance index (PSRI)	$\frac{R_{800}-R_{500}}{R_{750}}$
Jordan (1969b)	Ratio Vegetation Index (RVI)	$\frac{RED}{NIR}$
McFeeters (1996)	Normalized difference Water index (NDWI)	$\frac{GREEN-NIR}{GREEN+NIR}$
Gao (1996)	Normalized Difference Moisture Index (NDMI)	$\frac{NIR-SWIR}{NIR+SWIR}$
Tucker (1979)	Normalized Green Red Difference Index NGRDI	$\frac{GREEN-RED}{GREEN+RED}$
Goel and Qin (1994)	Non-Linear Index (NLI)	$\frac{NIR^2-RED}{NIR^2+RED}$
Gitelson et al. (2002)	Visible Atmospherically Resistant Index (VARI)	$\frac{GREEN-RED}{GREEN+RED-BLUE}$
Daughtry et al. (2000a)	Modified Chlorophyll Absorption in Reflectance Index (MCARI)	$[(R_{700} - R_{670}) - (0.2(R_{700} - R_{550})) \frac{R_{700}}{R_{670}}]$
Haboudane et al. (2002a)	Transformed Chlorophyll Absorption in Reflectance Index (TCARI)	$3[(R_{700} - R_{670}) - (0.2(R_{700} - R_{550})) \frac{R_{700}}{R_{670}}]$
Gamon et al. (1992)	Photochemical Reflectance Index (PRI)	$\frac{R_{831}-R_{670}}{R_{831}+R_{670}}$
Blackburn (1998)	Pigment Specific Simple Ratio (chlorophyll a) (PSSRa)	$\frac{R_{800}}{R_{680}}$
Blackburn (1998)	Pigment Specific Simple Ratio (chlorophyll b) (PSSRb)	$\frac{R_{800}}{R_{635}}$
Apan et al. (2004, 2003)	DSWI-1	$\frac{R800}{R1660}$
Apan et al. (2004, 2003)	DSWI-2	$\frac{R1660}{R550}$
Apan et al. (2004, 2003)	DSWI-3	$\frac{R1660}{R680}$
Apan et al. (2004, 2003)	DSWI-4	$\frac{R550}{R680}$
Apan et al. (2004, 2003)	DSWI-5	$\frac{R800+R550}{R1660+R680}$
Merzlyak et al. (1999a)	StructureInsensitive Pigment Index (SIPI)	$\frac{R_{800}-R_{445}}{R_{800}+R_{680}}$
Gitelson and Merzlyak (1994)	Simple Ratio (SR)	$\frac{R_{750}}{R_{705}}$
	SR 800/550	$\frac{R_{800}}{R_{550}}$
	Normalized Difference (ND) 750/660	$\frac{R_{750}-R_{660}}{R_{750}+R_{660}}$
Sims and Gamon (2002)	ND 800/680	$\frac{R_{800}-R_{680}}{R_{800}+R_{680}}$
Gitelson and Merzlyak (1994)	ND 750/705	$\frac{R_{750}-R_{705}}{R_{750}+R_{705}}$
Sims and Gamon (2002)	Modified SR (MSR)	$\frac{R_{750}-R_{445}}{R_{705}-R_{445}}$
Sims and Gamon (2002)	Modified ND (MND)	$\frac{R_{750}-R_{445}}{R_{750}+R_{705}-2R_{445}}$
Gitelson and Merzlyak (1994)	SR 750/550	$\frac{R_{750}}{R_{555}}$
	Ave(750–850)	Average between R_{750} and R_{850}
Daughtry et al. (2000b)	Modified Chlorophyll Absorption in Reflectance Index (MCARI)	$[(R_{700} - R_{670}) - 0.2(R_{700} - R_{550})) \frac{R_{700}}{R_{670}}$
Haboudane et al. (2002b)	Transformed Chlorophyll Absorption in Reflectance Index (TCARI)	$3[(R_{700} - R_{670}) - 0.2(R_{700} - R_{550})) \frac{R_{700}}{R_{670}}$
Rondeaux et al. (1996)	Optimized Soil-Adjusted Vegetation Index OSAVI	$(1 + 0.16) \frac{R_{800}-R_{670}}{R_{800}+R_{670}+0.16}$
Haboudane et al. (2002b)	Ratio TCARI/OSAVI	$\frac{TCARI}{OSAVI}$
Carter and Miller (1994)	SR 695/420	$\frac{R_{695}}{R_{420}}$
Carter and Miller (1994)	SR 695/760	$\frac{R_{695}}{R_{760}}$
Gitelson et al. (1996)	Green Normalized Difference Vegetation Index (GNDVI)	$\frac{(NIR-Green)}{(NIR+Green)}$
Gitelson and Merzlyak (1994)	Normalized Difference Red-edge Index (NDRE)	$\frac{(NIR-Red-edge)}{(NIR+Red-edge)}$
Gitelson et al. (2003)	Chlorophyll index – Green (CiGreen)	$\frac{NIR}{Green} - 1$
Gitelson et al. (2003)	Chlorophyll index – Red-edge (CiRE)	$\frac{NIR}{Red-edge} - 1$
Jordan (1969a)	Difference Vegetation Index (DVI)	$NIR - Red-edge$
Huete et al. (2002)	Enhanced Vegetation Index (EVI)	$2.5 \times \frac{(NIR-Red)}{(NIR+6 \times Red-7.5 \times Blue+1)}$
Vincini and Frazzi (2011)	Chlorophyll Vegetation Index (CVI)	$\frac{(NIR \times Red)}{Green^2}$
Broge and Leblanc (2001)	Triangular Vegetation Index (TVI)	$0.5 \times (120 \times (NIR - Green) - 200 \times (Red - Green))$
Merzlyak et al. (1999b)	Plant Senescence Reflectance Index (PSRI)	$\frac{(Red-Green)}{Red-edge}$
Zarco-Tejada et al. (2005)	Blue Green Pigment Index (BGI)	$\frac{Blue}{Green}$

(continued on next page)

Table 3 (continued).

Reference	Vegetation index	Formula
Louhaichi et al. (2001)	Green Leaf Index (GLI)	$\frac{(\text{Green}-\text{Red})+(\text{Green}-\text{Blue})}{(2 \times \text{Green} + \text{Red} + \text{Blue})}$
Qi et al. (1994)	Modified Soil Adjusted Vegetation Index (MSAVI)	$\frac{2\text{NIR}+1-\sqrt{(2\text{NIR}+1)^2-8(\text{NIR}-\text{RED})}}{2}$

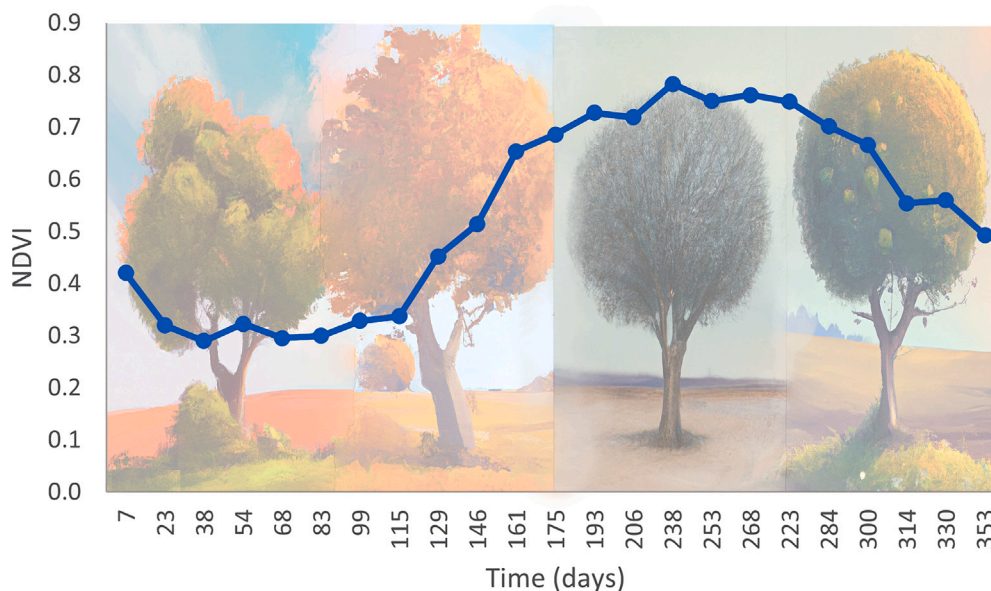


Fig. 4. NDVI measurements of sugarcane across entire growth cycle with MODIS and HJ-1 CCD remote sensing. Background images indicate approximate season. Source: Adapted from Chen et al. (2020) with Adobe Photoshop and AI generated artwork.

health monitoring systems, where a comprehensive understanding of environmental dynamics is crucial for accurate and reliable assessment of diseases.

7.3. Temporal morphological changes & multi-temporal analysis

Growth and maturation cause phenotypic and morphological changes in characteristics that dictate the spectral reflectance in sugarcane. This was investigated and observed in 25 sugarcane fields in Thailand with imagery from Landsat -8 OLI (Som-ard et al., 2021). Additionally, the average NDVI of the fields was observed to change over time, where phases associated with the largest amount of growth exhibited a higher NDVI (Som-ard et al., 2021). A similar result was obtained and observed to vary across sugarcane's lifecycle by Chen et al. (2020) with MODIS and HJ-1 CCD remote sensing, as can be seen in Fig. 4. Chen et al. (2020) observed that during the initial period from day 1 to 113, when vegetation coverage was sparse and soil was visible, NDVI values remained consistently low with minimal variation. A rapid increase in NDVI was observed between days 113 and 177, coinciding with the onset of stalk elongation. As the crop transitioned into the sugar accumulation stage between days 177 and 273, the rate of NDVI increase slowed. Following this, NDVI values began to decline as the plant entered its final maturation phase. Comparable results were then achieved in Indonesia by Susantoro et al. (2019).

Gers (2014, 2003) was able to distinguish phenological stages with multispectral imaging from Landsat 7, demonstrating that there is a significant difference in the spectral reflectance of sugarcane at different phenological stages. Additionally, temporal morphological changes indirectly contribute to the change in observed reflectance of sugarcane through flowering or lodging. This results from the reduction in the portion of canopy that is observable compared to soil, stalks and flowers, which exhibit different leaf orientation and cell structure (Berding and Hurney, 2005). Bégué et al. (2008) observed that the spectral

reflectance of sugarcane varied at an annual scale and concluded it is likely attributed to a combination of the topography and rainfall. These factors may need to be considered to accurately classify variation in spectral reflectance as a consequence of health conditions rather than seasonal changes.

The temporal aspect of sugarcane health monitoring has received limited research attention, with the majority of existing literature adopting a cross-sectional study approach (Apan et al., 2004, 2003; Moriya et al., 2017; Narmilan et al., 2022; Johansen et al., 2014; Simões and Rios do Amaral, 2023; Abdel-Rahman et al., 2010). The viability of producing a real-time sugarcane health monitoring system hinges on being able to detect health conditions for sugarcane across its life cycle with multi-temporal data. An investigation was conducted into this for disease detection in wheat by Franke and Menz (2007). Three separate multispectral images were captured at varying points in a wheat paddock across its life cycle. Spectral mixture analysis was performed and a decision tree was utilized to classify disease at various points in the wheat's life cycle with a classification accuracy of 56.8%, 65.9% and 88.6%. Younger crops have significantly smaller biomass, and therefore the reflectance will be more heavily influenced by the background soil as the composition of any given pixel will incorporate a larger percentage of soil (Alves Varella et al., 2015; Fang and Liang, 2014; Xue and Su, 2017). Additionally, the ML algorithm employed in this study has been superseded by newer tree-based models; implementing the more recently developed models could yield improved outcomes for health monitoring. Further studies should be conducted incorporating in situ soil reflectance measurements and vegetation indices into the models to observe the impact on results for large-scale disease detection in crops at early life cycle stages.

The study by Grisham et al. (2010) on SCYLV was the only known study to conduct multi-temporal disease detection in sugarcane using field spectroscopy. The results of this study demonstrate variation in spectral reflectance as a plant matures (Som-ard et al., 2021; Alves

Varella et al., 2015). This difference in spectral reflectance was observed to decrease between the collection of the first samples on the 13th of July and the second group of samples collected on the 12th of October. It was then observed in the samples collected on November 4th that the difference in spectral reflectance increased to approximately the same as seen in the July samples. The observed fluctuations in spectral reflectance differences over time suggest that distinct stages of the sugarcane life cycle may exhibit varying reactions to a disease. This temporal variation in spectral characteristics could potentially impact the accuracy of disease classification, as noted by Grisham et al. (2010), emphasizing the importance of understanding and accounting for temporal changes in sugarcane health monitoring. It would be beneficial to conduct further research into multi-temporal disease detection with spectral data to consolidate these findings.

7.4. Viewing angle of vegetation

An additional factor to consider in the development of a satellite-based real-time health monitoring system is the effects of viewing angle on spectral reflectance. Sugarcane like many other crops is non-Lambertian, and therefore a change in the viewing angles will influence the spectral reflectance. Moriya et al. (2018) investigated the effects of viewing angle variation in sugarcane radiometric measurements. They found a noticeable difference in the spectral reflectance profiles of sugarcane at different viewing angles (See Figure 3 in Moriya et al., 2018). The Bidirectional Reflectance Distribution Function (BRDF) correction model developed by Walthall et al. (1985) can be applied to compensate for the anisotropy factor. Specifically, Moriya et al. (2018) suggested that it could be utilized to correct hyperspectral images captured with an Unoccupied Aerial Vehicle (UAV) (Moriya et al., 2018). The BRDF correction model was utilized to calculate the spectral reflectance at different viewing angles (See Figure 6 in Moriya et al., 2018). Moriya et al. (2017) used the BRDF correction for sugarcane health monitoring and was the only health monitoring study which considered the effect of viewing angle. Future research should ensure spectral images are centred at a consistent location and viewing angle. Additionally, the BRDF correction model should be considered to handle the anisotropy factor.

8. Machine learning algorithms and methods of analysis

For large-scale sugarcane health monitoring, the common theme amongst current literature is the use of ML algorithms for classification of the plant health into healthy or unhealthy states (Apan et al., 2004, 2003; Moriya et al., 2017; Narmilan et al., 2022; Johansen et al., 2014; Simões and Rios do Amaral, 2023; Ong et al., 2023). Numerous ML methods can be undertaken to solve this classification problem, in depth details of these algorithms can be found in relevant textbooks (Cerulli, 2023). Table 1 provides details of multispectral and hyperspectral studies in the literature and shows various ML algorithms used in them.

The study by Apan et al. (2004, 2003) classifies orange rust disease in sugarcane exclusively using stepwise Linear Discriminant Analysis (LDA) with vegetation indices as features. This produced a classification accuracy of 96.9% with the linear combination of DSWI-2, SR695/420, and NDWI-Hyp. This demonstrates that ML algorithms can be effective in classifying the disease state of sugarcane. However, Apan et al. (2004, 2003) did not compare the effectiveness of different ML algorithms for satellite disease detection, which can be of significance as indicated by other disease detection papers (Narmilan et al., 2022; Franke and Menz, 2007; Simões and Rios do Amaral, 2023; Ong et al., 2023). Additionally, Apan et al. (2004, 2003) concluded that future studies should be conducted to determine the viability of disease detection in the early stages. A simplified visualization of the methodology used by Apan et al. (2004, 2003) can be seen in Fig. 5. The figure demonstrates an appropriate overarching approach to sugarcane health

monitoring with spectroscopy and ML, in which LDA can be replaced with other ML algorithms.

Several recent studies have made strides in evaluating the effectiveness of various ML algorithms for disease detection in sugarcane. Notably, Random Forest and Radial SVM consistently emerged as top performers (Narmilan et al., 2022; Simões and Rios do Amaral, 2023; Ong et al., 2023). However, it is important to note that the number of studies comparing ML algorithms in this context remains somewhat limited, making it challenging to pinpoint the precise factors contributing to the superior efficacy of a particular method. In a similar vein, Everingham et al. (2007), while investigating different ML algorithms to discern various sugarcane varieties based on their hyperspectral reflectance, found that SVM and Random Forest consistently outperformed other methods. While these findings are still in their early stages, the emergence of Random Forest and Radial SVM as potent tools for health monitoring in sugarcane suggests that non-linear classifiers hold great promise. These classifiers excel at capturing complex patterns and relationships within the data, hinting at the potential for more accurate and robust disease detection systems as this field of research continues to evolve.

ML algorithms utilized in this context exhibit considerable variability, leading to diverse classification results. For instance, Apan et al. (2003) employed LDA achieving a classification accuracy of 96.9%. The effectiveness of LDA hinges on assumptions related to the linearity and separability of spectral data and vegetation indices. However, these assumptions may not consistently hold across different diseases or datasets, and may require statistical analysis to assess whether the data meets the necessary assumptions for LDA implementation (James et al., 2013; Johnson and Wichern, 2014). Evaluating the performance of LDA against other models like QDA or SVM with non-linear kernels could shed light on the linear separability of the data. It is very improbable that there is a single ML algorithm that will consistently outperform all others for all classification tasks related to sugarcane health monitoring, and consequently the specific characteristics and underlying distributions of the data should be analysed when specifying a desired approach or commenting on its performance. Future studies should transparently present underlying distributions of their data and conduct thorough comparisons of multiple ML algorithms based on these characteristics. Furthermore, in alignment with best practices for any ML project, rigorous feature selection procedures should be conducted to ascertain the importance of predictors.

Moriya et al. (2017) took a different approach utilizing Spectral Information Divergence (SID) to classify mosaic virus in sugarcane from drone-based hyperspectral images achieving a classification accuracy of 92%. In two instances of implementing Decision Tree (DT) classifiers (Narmilan et al., 2022; Franke and Menz, 2007), sub-optimal performance was exhibited in general or when compared to alternative tree-based methods. Newer alternative tree-based models, such as eXtreme Gradient Boosting (XGB) and Random Forest (RF), should be considered for enhanced accuracy and robustness in sugarcane health monitoring systems. Alternatively, the only other study to develop a DT classifier did not perform cross-validation which is vital to corroborate the effectiveness of the classification method (Dutia et al., 2006). Despite the widespread application of neural networks in precision agriculture, only two papers at the time of writing implemented a neural network for sugarcane health monitoring with spectroscopy data (Bao et al., 2021, 2024). Future investigations may benefit from further exploring the capabilities and advantages that neural networks could bring to this domain.

Several studies analysed the underlying distributions of the data and performed a more traditional statistical analysis of the differences between diseased and healthy sugarcane. Canonical Discriminant Analysis (CDA) was implemented by Abdel-Rahman et al. (2010) and determined that there is a statistically significant difference in the hyperspectral reflectance of Thrips damaged crops compared to healthy crops. A comparable statistical analysis was performed on the spectral

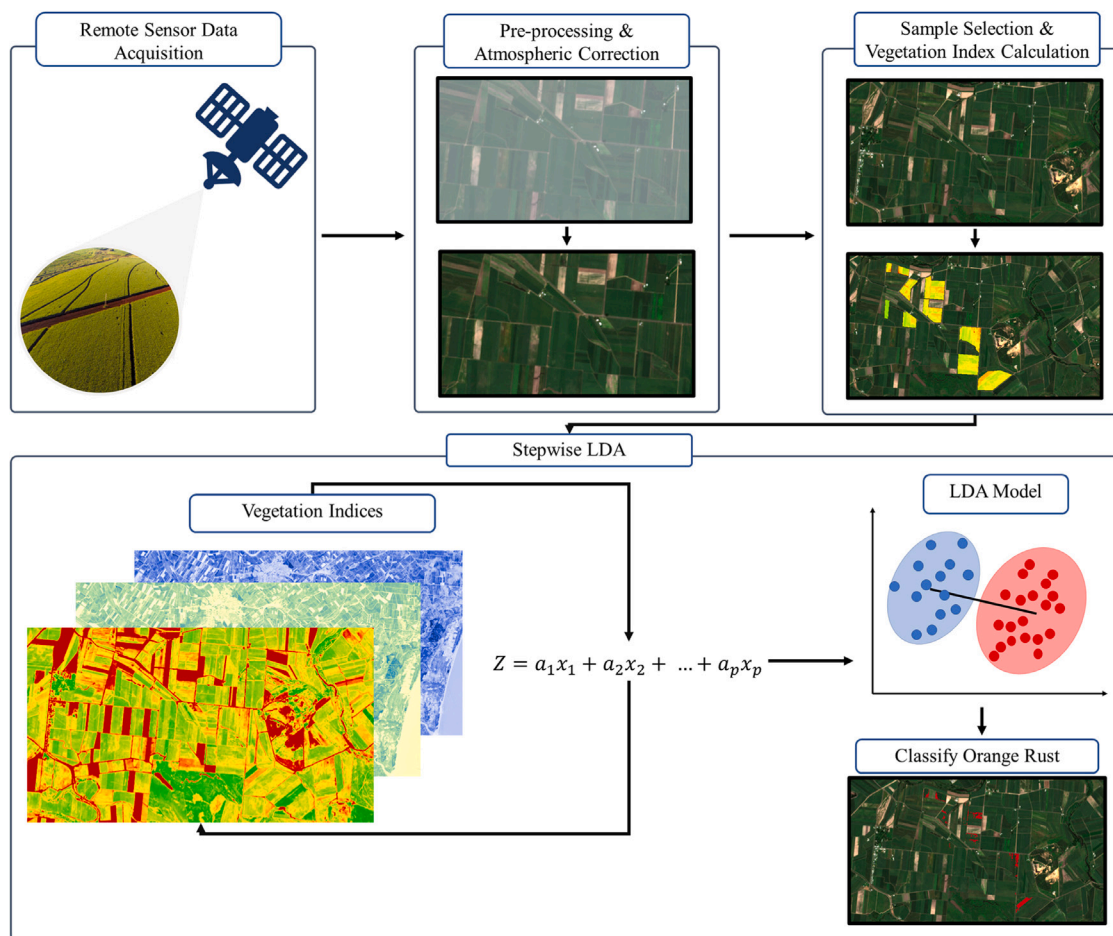


Fig. 5. Visualization of Apan et al. (2004, 2003) methodology to classify Orange Rust disease from EO-1 Hyperion images in Mackay, Australia with stepwise LDA.

reflectance observed with a laboratory-based spectrometer of sugarcane with Brown and Orange Rust by Soca-Muñoz et al. (2020) demonstrating 11.9% and 9.9% differences in the vegetation indices NDVI and ENVI respectively.

9. Conclusion and future work

In this study, we reviewed factors, identified in the literature, that affect the accuracy of large-scale sugarcane health monitoring, and hence need to be considered in the development of a large-scale sugarcane health monitoring system. This included sugarcane growth factors, vegetation indices, specifications of the satellite-based spectroscopy, factors that influence the observed reflectance of sugarcane, and ML algorithms utilized in the analysis. To date, there is limited literature pertaining to a system of this nature and several gaps have been identified for future research.

A large portion of the current hyperspectral sugarcane health monitoring has been conducted with field spectroscopy with limited use for a large-scale solution for sugarcane farmers. Despite current literature discussing the effectiveness of spectroscopy to detect sugarcane disease/pest, they typically lack a comparison of ML algorithms to indicate the most effective classifier for this application. Furthermore, a large portion of known sugarcane health conditions have yet to be detected with newer techniques or systems. There is currently no literature addressing the possibility of classifying diseases and pests at different points in the sugarcane life cycle with satellite-based multi-temporal data.

A characteristic vital to an effective sugarcane health monitoring system is the ability to detect and/or identify multiple diseases, pests, and varieties, simultaneously. Currently, there is limited literature demonstrating this with any form of spectral imaging for sugarcane. The current literature indicates the plausibility of a satellite-based health monitoring system. However, to achieve such a system, several gaps in the literature need to be addressed before the commencement of development. Several recommendations have been made for future studies to fill these gaps.

- A practical solution to a large-scale sugarcane health monitoring system will need to be capable of identifying a larger number of health conditions simultaneously. The effectiveness of satellite-based spectroscopy for health monitoring should be evaluated for impactful sugarcane diseases yet to be considered, which include but are not limited to, Sereh, Red Rot, RSD, Smut, Pachymetra, Chlorotic Streak, Yellow Spot, and Fiji Leaf Gall.
- A wide variety of different sugarcane varieties are utilized worldwide depending on the climate. An ideal large-scale sugarcane health monitoring system will need to be capable of identifying the aforementioned health conditions for all of the most prominent sugarcane varieties by considering the variation in their spectral reflectance. The effectiveness of satellite-based spectroscopy for this should be evaluated to indicate if region-specific health monitoring systems and models are required based on the local sugarcane varieties.
- Future studies should move beyond the prevailing focus on raw spectral measurements or limited use of vegetation indices considering the demonstrated success of studies that incorporate

multiple vegetation indices into their models. Success with vegetation indices indicating variation in moisture content indicates that their inclusion in future studies and systems should be contemplated.

- Further studies should investigate and perform a direct comparison of disease classification effectiveness with satellite-based spectroscopy and drone-based spectroscopy, to indicate trade-offs in accuracy and real-world logistical consequences associated with each method.
- Models for classifying health conditions need to consider the environmental and meteorological variations. Current studies often overlook the influence of annual weather fluctuations, including temperature, humidity, sunlight duration, wind patterns, and precipitation. A comprehensive investigation into how these variations impact the effectiveness of health monitoring methods and understanding the interplay between environmental factors and ML models will contribute to the reliability of sugarcane health assessments.
- Increasing the chance of early detection of health conditions is vital for reducing the spread or progression of the condition. Therefore, it would be valuable to develop and evaluate the effectiveness of models capable of time series disease detection for prominent sugarcane varieties and diseases. Furthermore, evaluating how the different life cycle stages of sugarcane affect disease detection and the prevalence of exposed soil should be considered.
- Given the diverse nature of sugarcane health monitoring tasks and datasets, a one-size-fits-all ML algorithm is improbable. Future studies should carefully analyse specific characteristics of their dataset, transparently report distributions, and conduct thorough comparisons among multiple algorithms to identify the most suitable approach. Rigorous feature selection is essential to ensure the relevance and impact of predictors in enhancing model performance.
- Neural networks and deep learning have shown unparalleled performance in various applications. Future research can develop new neural networks for sugarcane health monitoring and compare them with the most effective ML algorithms for health monitoring and variety classification.
- To incentivize widespread adoption of the discussed precision agriculture monitoring technology, it would be desirable to utilize freely available satellites. However, freely available satellites typically have a worse spectral and spatial resolution in comparison to drones or commercial satellites. To determine how much uncertainty is introduced through the utilization of satellite-based spectroscopy rather than the superior spatial resolution of drone-based spectroscopy, both methods should be compared and analysed. Furthermore, the minimum spatial and spectral resolutions required to develop a large-scale health monitoring system should be determined so that the running and production costs of this system can be reduced where possible.
- Developing software to automatically acquire satellite images, calculate vegetation indices, and detect disease in sugarcane, displaying the results to a user on a simple user interface and dashboard is another valuable research and development direction. The development of a program that is easy to use would be vital for increasing the probability of its adoption in the industry.
- Performing a cost analysis of the sugarcane industry's current health monitoring practices against the proposed large-scale health monitoring system with freely or commercially available satellites would also be essential for adoption and practice changes.

CRediT authorship contribution statement

Ethan Kane Waters: Writing – review & editing, Writing – original draft, Visualization, Methodology, Investigation, Data curation, Conceptualization. **Carla Chia-Ming Chen:** Writing – review & editing, Supervision. **Mostafa Rahimi Azghadi:** Writing – review & editing, Supervision, Conceptualization.

Declaration of Generative AI and AI-assisted technologies in the writing process

During the preparation of this work the author(s) used DALL-E 2 in order to contribute towards visualization. After using this tool/service, the author(s) reviewed and edited the content as needed and take(s) full responsibility for the content of the publication.

Funding

This work was supported by Australia's Economic Accelerator Seed grant provided by the Australian Government, Department of Education.

Declaration of competing interest

The authors declare that they have no known competing financial interests or personal relationships that could have appeared to influence the work reported in this paper.

Data availability

No data was used for the research described in the article.

References

- Abdel-Rahman, E., Ahmed, F., van den Berg, M., Way, M., 2010. Potential of spectroscopic data sets for sugarcane thrips (*fulmekiola serrata kobus*) damage detection. *Int. J. Remote Sens.* 31, 4199–4216. <http://dx.doi.org/10.1080/01431160903241981>.
- Agapiou, A., Hadjimitsis, D.G., Papoutsas, C., Alexakis, D.D., Papadavid, G., 2011. The importance of accounting for atmospheric effects in the application of NDVI and interpretation of satellite imagery supporting archaeological research: The case studies of palaepaphos and nea paphos sites in cyprus. *Remote Sens.* 3 (12), 2605–2629. <http://dx.doi.org/10.3390/rs3122605>.
- Agnihotri, V.P., 1983. Diseases of sugarcane. *Dis. Sugarcane*.
- Alves Varella, C.A., Gleriani, J.M., dos Santos, R.M., 2015. Precision agriculture and remote sensing. In: *Sugarcane*. Academic Press, San Diego, pp. 185–203. <http://dx.doi.org/10.1016/B978-0-12-802239-9.00009-8>.
- Apan, A., Held, A., Phinn, S., Markley, J., 2003. Formulation and assessment of narrow-band vegetation indices from EO1 hyperion imagery for discriminating sugarcane disease. In: *Proceedings of the Spatial Sciences Conference*.
- Apan, A., Held, A., Phinn, S., Markley, J., 2004. Detecting sugarcane 'orange rust' disease using EO-1 hyperion hyperspectral imagery. *Int. J. Remote Sens.* 25 (2), 489–498. <http://dx.doi.org/10.1080/01431160310001618031>.
- Baghdadi, N., Boyer, N., Todoroff, P., El Hajj, M., Bégué, A., 2009. Potential of SAR sensors TerraSAR-X, ASAR/ENVISAT and PALSAR/ALOS for monitoring sugarcane crops on reunion island. *Remote Sens. Environ.* 113 (8), 1724–1738. <http://dx.doi.org/10.1016/j.rse.2009.04.005>, URL: <https://www.sciencedirect.com/science/article/pii/S0034425709001229>.
- Bailey, R., Bechet, G., 1986. Effect of ratoon stunting disease on the yield and components of yield of sugarcane under rainfed conditions. In: *Proceedings of the South African Sugar Technologists Association*, vol. 60, pp. 204–210.
- Bao, D., Zhou, J., Bhuiyan, S.A., Adhikari, P., Tuxworth, G., Ford, R., Gao, Y., 2024. Early detection of sugarcane smut and mosaic diseases via hyperspectral imaging and spectral-spatial attention deep neural networks. *J. Agric. Food Res.* 18, 101369. <http://dx.doi.org/10.1016/j.jafr.2024.101369>, URL: <https://www.sciencedirect.com/science/article/pii/S266615432400406X>.
- Bao, D., Zhou, J., Bhuiyan, S.A., Zia, A., Ford, R., Gao, Y., 2021. Early detection of sugarcane smut disease in hyperspectral images. In: 2021 36th International Conference on Image and Vision Computing New Zealand. IVCNZ, pp. 1–6. <http://dx.doi.org/10.1109/IVCNZ54163.2021.9653386>.

- Bégué, A., Todoroff, P., Pater, J., 2008. Multi-time scale analysis of sugarcane within-field variability: improved crop diagnosis using satellite time series? *Precis. Agric.* 9, 161–171. <http://dx.doi.org/10.1007/s11119-008-9063-3>.
- Berding, N., Hurney, A.P., 2005. Flowering and lodging, physiological-based traits affecting cane and sugar yield: What do we know of their control mechanisms and how do we manage them? *Field Crops Res.* 92 (2), 261–275. <http://dx.doi.org/10.1016/j.fcr.2005.01.015>.
- Blackburn, G.A., 1998. Spectral indices for estimating photosynthetic pigment concentrations: A test using senescent tree leaves. *Int. J. Remote Sens.* 19 (4), 657–675. <http://dx.doi.org/10.1080/014311698215919>.
- Brandes, E., et al., 1920. Artificial and insect transmission of sugarcane mosaic. *J. Agric. Res.* 19 (3), 131–8.
- Broge, N., Leblanc, E., 2001. Comparing prediction power and stability of broadband and hyperspectral vegetation indices for estimation of green leaf area index and canopy chlorophyll density. *Remote Sens. Environ.* 76 (2), 156–172. [http://dx.doi.org/10.1016/S0034-4257\(00\)00197-8](http://dx.doi.org/10.1016/S0034-4257(00)00197-8).
- Canata, T.F., Wei, M.C.F., Maldaner, L.F., Molin, J.P., 2021. Sugarcane yield mapping using high-resolution imagery data and machine learning technique. *Remote Sens.* 13 (2), <http://dx.doi.org/10.3390/rs13020232>, URL: <https://www.mdpi.com/2072-4292/13/2/232>.
- Canegrowers, 2019. Annual Report. Report, Canegrowers.
- Carter, G.A., Miller, R.L., 1994. Early detection of plant stress by digital imaging within narrow stress-sensitive wavebands. *Remote Sens. Environ.* 50 (3), 295–302. [http://dx.doi.org/10.1016/0034-4257\(94\)90079-5](http://dx.doi.org/10.1016/0034-4257(94)90079-5), URL: <https://www.sciencedirect.com/science/article/pii/0034425794900795>.
- Carvalho, G., da Silva, T., Munhoz, A., Monteiro-Vitorello, C., Azevedo, R., Melotto, M., Camargo, L., 2016. Development of a qPCR for *Leifsonia xyli* subsp. *xyli* and quantification of the effects of heat treatment of sugarcane cuttings on Lxx. *Crop Prot.* 80, 51–55. <http://dx.doi.org/10.1016/j.cropro.2015.10.029>.
- Cerulli, G., 2023. Fundamentals of Supervised Machine Learning With Applications in Python, R, and Stata. Springer Cham, <http://dx.doi.org/10.1007/978-3-031-41337-7>.
- Chen, Y., Feng, L., Mo, J., Mo, W., Ding, M., Liu, Z., 2020. Identification of sugarcane with NDVI time series based on HJ-1 CCD and MODIS fusion. *J. Indian Soc. Remote Sens.* 48 (2), 249–262. <http://dx.doi.org/10.1007/s12524-019-01042-1>.
- Daughtry, C., Walthall, C., Kim, M., de Colstoun, E., McMurtrey, J., 2000a. Estimating corn leaf chlorophyll concentration from leaf and canopy reflectance. *Remote Sens. Environ.* 74 (2), 229–239. [http://dx.doi.org/10.1016/S0034-4257\(00\)00113-9](http://dx.doi.org/10.1016/S0034-4257(00)00113-9).
- Daughtry, C., Walthall, C., Kim, M., de Colstoun, E., McMurtrey, J., 2000b. Estimating corn leaf chlorophyll concentration from leaf and canopy reflectance. *Remote Sens. Environ.* 74 (2), 229–239. [http://dx.doi.org/10.1016/S0034-4257\(00\)00113-9](http://dx.doi.org/10.1016/S0034-4257(00)00113-9), URL: <https://www.sciencedirect.com/science/article/pii/S0034425700001139>.
- Davis, M.J., Gillaspie, A.G., Vidaver, A.K., Harris, R.W., 1984. *Clavibacter*: a new genus containing some phytopathogenic coryneform bacteria, including *Clavibacter xyli* subsp. *xyli* sp. nov., subsp. nov. and *Clavibacter xyli* subsp. *cynodontis* subsp. nov., pathogens that cause ratoon stunting disease of sugarcane and bermudagrass stunting disease†. *Int. J. Syst. Evol. Microbiol.* 34 (2), 107–117. <http://dx.doi.org/10.1099/00207713-34-2-107>.
- de França e Silva, N.R., Chaves, M.E.D., Luciano, A.C.d.S., Sanches, I.D., de Almeida, C.M., Adami, M., 2024. Sugarcane yield estimation using satellite remote sensing data in empirical or mechanistic modeling: A systematic review. *Remote Sens.* 16 (5), 863.
- de los Reyes, R., Langheinrich, M., Schwind, P., Richter, R., Pflug, B., Bachmann, M., Müller, R., Carmona, E., Zekoll, V., Reinartz, P., 2020. PACO: Python-based atmospheric correction. *Sensors* 20 (5), <http://dx.doi.org/10.3390/s20051428>.
- de S. Rossato, Jr., J.A., Costa, G.H.G., Madaleno, L.L., Mutton, M.J.R., Higley, L.G., Fernandes, O.A., 2013. Characterization and impact of the sugarcane borer on sugarcane yield and quality. *Agron. J.* 105 (3), 643–648. <http://dx.doi.org/10.2134/agronj2012.0309>.
- Duft, D., Luciano, A., Fiorio, P., 2019. Sentinel-2B and random forest algorithm potential for sugarcane varieties identification. In: *Proceedings of XX Brazilian Symposium on Geoinformatics*. pp. 188–193.
- Dutia, S., Bhattacharya, B., Rajak, D., Chattopadhyay, C., and, N., Parihar, J., 2006. Disease detection in mustard crop using EO-1 hyperion satellite data. *J. Indian Soc. Remote Sens.* (Photonirvachak) 34.
- ElMasry, G., Sun, D.W., 2010. CHAPTER 1 - principles of hyperspectral imaging technology. In: Sun, D.-W. (Ed.), *Hyperspectral Imaging for Food Quality Analysis and Control*. Academic Press, San Diego, pp. 3–43. <http://dx.doi.org/10.1016/B978-0-12-374753-2.10001-2>.
- Emick, E., Babcock, C., White, G.W., Hudak, A.T., Domke, G.M., Finley, A.O., 2023. An approach to estimating forest biomass while quantifying estimate uncertainty and correcting bias in machine learning maps. *Remote Sens. Environ.* 295, 113678. <http://dx.doi.org/10.1016/j.rse.2023.113678>.
- European Space Agency, 2022a. Earth observing 1. <https://www.eoportal.org/satellite-missions/eo-1>. (Accessed 01 May 2022).
- European Space Agency, 2022b. PROBA-1. <https://earth.esa.int/eogateway/missions/proba-1?text=Proba-1>. (Accessed 01 May 2022).
- European Space Agency, 2022c. QuickBird-2. <https://earth.esa.int/eogateway/missions/quickbird-2>. (Accessed 01 May 2022).
- European Space Agency, 2022d. Sentinel-2 overview. <https://sentinels.copernicus.eu/web/sentinel/missions/sentinel-2/overview>. (Accessed 01 May 2022).
- European Space Agency, 2022e. SPOT 6 and 7 ESA archive. <https://earth.esa.int/eogateway/catalog/spot-6-and-7-esa-archive?text=spot+6>. (Accessed 01 May 2022).
- Everingham, Y., Lowe, K.H., Donald, D., Coomans, D., Markley, J., 2007. Advanced satellite imagery to classify sugarcane crop characteristics. *Agron. Sustain. Dev.* 27, <http://dx.doi.org/10.1051/agro:2006034>.
- Everingham, Y., Sexton, J., Skocaj, D., Inman-Bamber, G., 2016. Accurate prediction of sugarcane yield using a random forest algorithm. *Agron. Sustain. Dev.* 36, 1–9.
- Fang, H., Liang, S., 2014. Leaf area index models. In: *Reference Module in Earth Systems and Environmental Sciences*. ISBN: 978-0-12-409548-9, <http://dx.doi.org/10.1016/B978-0-12-409548-9.09076-X>.
- Fegan, M., Croft, B.J., Teakle, D.S., Hayward, A.C., Smith, G.R., 1998. Sensitive and specific detection of *Clavibacter xyli* subsp. *xyli*, causal agent of ratoon stunting disease of sugarcane, with a polymerase chain reaction-based assay. *Plant Pathol.* 47 (4), 495–504. <http://dx.doi.org/10.1046/j.1365-3059.1998.00255.x>.
- Feng, X., He, L., Cheng, Q., Long, X., Yuan, Y., 2020. Hyperspectral and multispectral remote sensing image fusion based on endmember spatial information. *Remote Sens.* 12 (6), 1009. <http://dx.doi.org/10.3390/rs12061009>.
- Fernandes, J.L., Ebecken, N.F.F., Esquerdo, J.C.D.M., 2017. Sugarcane yield prediction in Brazil using NDVI time series and neural networks ensemble. *Int. J. Remote Sens.* 38 (16), 4631–4644.
- Food and Agriculture Organization of the United Nations, 2023. Production / Crops and livestock products - Metadata. Food and Agriculture Organization of the United Nations (FAO), URL: <https://www.fao.org/faostat/en/#data/QCL>.
- Franke, J., Menz, G., 2007. Multi-temporal wheat disease detection by multi-spectral remote sensing. *Precis. Agric.* 8 (3), 161–172. <http://dx.doi.org/10.1007/s11119-007-9036-y>.
- Galeazzi, C., Sacchetti, A., Cisbani, A., Babini, G., 2008. The PRISMA program. In: *IGARSS 2008 - 2008 IEEE International Geoscience and Remote Sensing Symposium*, vol. 4, pp. IV – 105–IV – 108. <http://dx.doi.org/10.1109/IGARSS.2008.4779667>.
- Galvão, L.S., Formaggio, A.R., Tisot, D.A., 2005. Discrimination of sugarcane varieties in southeastern Brazil with EO-1 hyperion data. *Remote Sens. Environ.* 94 (4), 523–534. <http://dx.doi.org/10.1016/j.rse.2004.11.012>.
- Galvão, L.S., Formaggio, A.R., Tisot, D.A., 2006. The influence of spectral resolution on discriminating Brazilian sugarcane varieties. *Int. J. Remote Sens.* 27 (4), 769–777. <http://dx.doi.org/10.1080/01431160500166011>.
- Gamon, J., Peñuelas, J., Field, C., 1992. A narrow-waveband spectral index that tracks diurnal changes in photosynthetic efficiency. *Remote Sens. Environ.* 41 (1), 35–44. [http://dx.doi.org/10.1016/0034-4257\(92\)90059-5](http://dx.doi.org/10.1016/0034-4257(92)90059-5).
- Gao, B.c., 1996. NDWI—A normalized difference water index for remote sensing of vegetation liquid water from space. *Remote Sens. Environ.* 58 (3), 257–266. [http://dx.doi.org/10.1016/S0034-4257\(96\)00067-3](http://dx.doi.org/10.1016/S0034-4257(96)00067-3).
- García, A.P., Umezú, C.K., Polania, E.C.M., Dias Neto, A.F., Rossetto, R., Albiero, D., 2022. Sensor-based technologies in sugarcane agriculture. *Sugar Tech* 24 (3), 679–698.
- Genc, H., Genc, L., Turhan, H., Smith, S., Nation, J., 2008. Vegetation indices as indicators of damage by the sunn pest (Hemiptera: Scutelleridae) to field grown wheat. *Afr. J. Biotechnol.* 7 (2).
- Gers, C.J., 2003. Remotely sensed sugarcane phenological characteristics at Umfolozi South Africa. In: *IGARSS 2003. 2003 IEEE International Geoscience and Remote Sensing Symposium. Proceedings (IEEE Cat. No.03CH37477)*, vol. 2, pp. 1010–1012. <http://dx.doi.org/10.1109/IGARSS.2003.1293995>.
- Gers, C., 2014. Relating remotely sensed multi-temporal landsat 7 ETM+ imagery to sugarcane characteristics. In: *Proc S Afr Sug Technol Ass. Citeseer*, p. 7.
- Ghai, M., Singh, V., Martin, L., McFarlane, S., van Antwerpen, T., Rutherford, R., 2014. A rapid and visual loop-mediated isothermal amplification assay to detect *Leifsonia xyli* subsp. *xyli* targeting a transposase gene. *Lett. Appl. Microbiol.* 59 (6), 648–657. <http://dx.doi.org/10.1111/lam.12327>.
- Gitelson, A.A., Gritz, Y., Merzlyak, M.N., 2003. Relationships between leaf chlorophyll content and spectral reflectance and algorithms for non-destructive chlorophyll assessment in higher plant leaves. *J. Plant Physiol.* 160 (3), 271–282. <http://dx.doi.org/10.1078/0176-1617-00887>, URL: <https://www.sciencedirect.com/science/article/pii/S0176161704704034>.
- Gitelson, A.A., Kaufman, Y.J., Merzlyak, M.N., 1996. Use of a green channel in remote sensing of global vegetation from EOS-MODIS. *Remote Sens. Environ.* 58 (3), 289–298. [http://dx.doi.org/10.1016/S0034-4257\(96\)00072-7](http://dx.doi.org/10.1016/S0034-4257(96)00072-7), URL: <https://www.sciencedirect.com/science/article/pii/S0034425796000727>.
- Gitelson, A.A., Kaufman, Y.J., Stark, R., Rundquist, D., 2002. Novel algorithms for remote estimation of vegetation fraction. *Remote Sens. Environ.* 80 (1), 76–87.
- Gitelson, A., Merzlyak, M.N., 1994. Quantitative estimation of chlorophyll-a using reflectance spectra: Experiments with autumn chestnut and maple leaves. *J. Photochem. Photobiol. B: Biol.* 22 (3), 247–252. [http://dx.doi.org/10.1016/1011-1344\(93\)06963-4](http://dx.doi.org/10.1016/1011-1344(93)06963-4), URL: <https://www.sciencedirect.com/science/article/pii/1011134493069634>.

- Godfray, H.C.J., Beddington, J.R., Crute, I.R., Haddad, L., Lawrence, D., Muir, J.F., Pretty, J., Robinson, S., Thomas, S.M., Toulmin, C., 2010. Food security: The challenge of feeding 9 billion people. *Science* 327 (5967), 812–818. <http://dx.doi.org/10.1126/science.1185383>.
- Goel, N.S., Qin, W., 1994. Influences of canopy architecture on relationships between various vegetation indices and LAI and Fpar: A computer simulation. *Remote Sens. Rev.* 10 (4), 309–347. <http://dx.doi.org/10.1080/02757259409532252>.
- Goetz, A.F.H., Vane, G., Solomon, J.E., Rock, B.N., 1985. Imaging spectrometry for earth remote sensing. *Science* 228 (4704), 1147–1153. <http://dx.doi.org/10.1126/science.228.4704.1147>.
- Gregory, P.J., George, T.S., 2011. Feeding nine billion: the challenge to sustainable crop production. *J. Exp. Bot.*
- Grisham, M.P., Johnson, R.M., Zimba, P.V., 2010. Detecting sugarcane yellow leaf virus infection in asymptomatic leaves with hyperspectral remote sensing and associated leaf pigment changes. *J. Virol. Methods* 167 (2), <http://dx.doi.org/10.1016/j.jviromet.2010.03.024>, 140–5.
- Guzmán Q., J.A., Pinto-Ledezma, J.N., Frantz, D., Townsend, P.A., Juzwik, J., Cavender-Bares, J., 2023. Mapping oak wilt disease from space using land surface phenology. *Remote Sens. Environ.* 298, 113794. <http://dx.doi.org/10.1016/j.rse.2023.113794>.
- Haboudane, D., Miller, J.R., Tremblay, N., Zarco-Tejada, P.J., Dextraze, L., 2002a. Integrated narrow-band vegetation indices for prediction of crop chlorophyll content for application to precision agriculture. *Remote Sens. Environ.* 81 (2), 416–426. [http://dx.doi.org/10.1016/S0034-4257\(02\)00018-4](http://dx.doi.org/10.1016/S0034-4257(02)00018-4).
- Haboudane, D., Miller, J.R., Tremblay, N., Zarco-Tejada, P.J., Dextraze, L., 2002b. Integrated narrow-band vegetation indices for prediction of crop chlorophyll content for application to precision agriculture. *Remote Sens. Environ.* 81 (2), 416–426. [http://dx.doi.org/10.1016/S0034-4257\(02\)00018-4](http://dx.doi.org/10.1016/S0034-4257(02)00018-4), URL: <https://www.sciencedirect.com/science/article/pii/S0034425702000184>.
- Hadjimitsis, D., Clayton, C., Retalis, A., 2003. On the darkest pixel atmospheric correction algorithm: A revised procedure applied over satellite remotely sensed images intended for environmental applications. *Proc. SPIE - Int. Soc. Opt. Eng.* 5239, 464–471. <http://dx.doi.org/10.1117/12.511520>.
- Hadjimitsis, D.G., Papadavid, G., Agapiou, A., Themistocleous, K., Hadjimitsis, M.G., Retalis, A., Michaelides, S., Chrysoulakis, N., Toullos, L., Clayton, C.R.I., 2010. Atmospheric correction for satellite remotely sensed data intended for agricultural applications: impact on vegetation indices. *Nat. Hazards Earth Syst. Sci.* 10 (1), 89–95. <http://dx.doi.org/10.5194/nhess-10-89-2010>.
- Hapke, B., 1981. Bidirectional reflectance spectroscopy: 1. Theory. *J. Geophys. Res.: Solid Earth* 86 (B4), 3039–3054. <http://dx.doi.org/10.1029/JB086iB04p03039>.
- Hapke, B., Wells, E., 1981. Bidirectional reflectance spectroscopy: 2. Experiments and observations. *J. Geophys. Res.: Solid Earth* 86 (B4), 3055–3060. <http://dx.doi.org/10.1029/JB086iB04p03055>.
- Hensley, S.D., 1971. Management of sugarcane borer populations in Louisiana, a decade of change. *Entomophaga* 16, 133–146. <http://dx.doi.org/10.1007/BF02370696>.
- Hong, Y., Xie, T., Luo, L., Wang, M., Li, D., Zhang, Q., Xu, T., 2024. Area extraction and growth monitoring of sugarcane from multi-source remote sensing images under a polarimetric SAR data compensation based on buildings. *Geo-spatial Inf. Sci.* 1–18. <http://dx.doi.org/10.1080/10095020.2024.2381607>.
- Huete, A., Didan, K., Miura, T., Rodriguez, E., Gao, X., Ferreira, L., 2002. Overview of the radiometric and biophysical performance of the MODIS vegetation indices. *Remote Sens. Environ.* 83 (1), 195–213. [http://dx.doi.org/10.1016/S0034-4257\(02\)00096-2](http://dx.doi.org/10.1016/S0034-4257(02)00096-2), The Moderate Resolution Imaging Spectroradiometer (MODIS): a new generation of Land Surface Monitoring.
- Hunt, E., Rock, B.N., 1989. Detection of changes in leaf water content using near- and middle-infrared reflectances. *Remote Sens. Environ.* 30 (1), 43–54. [http://dx.doi.org/10.1016/0034-4257\(89\)90046-1](http://dx.doi.org/10.1016/0034-4257(89)90046-1).
- Ientilucci, E.J., Adler-Golden, S., 2019. Atmospheric compensation of hyperspectral data: An overview and review of in-scene and physics-based approaches. *IEEE Geosci. Remote Sens. Mag.* 7 (2), 31–50. <http://dx.doi.org/10.1109/MGRS.2019.2904706>.
- James, G., Witten, D., Hastie, T., Tibshirani, R., 2013. Classification. In: *An Introduction to Statistical Learning: With Applications in R*. Springer New York, New York, NY, pp. 127–173. http://dx.doi.org/10.1007/978-1-4614-7138-7_4.
- Johansen, K., Robson, A., Samson, P., Sallam, N., Chandler, K., Eaton, A., Derby, L., Jennings, J., 2014. Mapping canegrub damage from high spatial resolution satellite imagery. In: *Proceedings of the 36th Conference of the Australian Society of Sugar Cane Technologists*. ASSCT 2014, pp. 62–70.
- Johansen, K., Sallam, N., Robson, A., Samson, P., Chandler, K., Derby, L., Eaton, A., Jennings, J., 2018. Using GeoEye-1 imagery for multi-temporal object-based detection of canegrub damage in sugarcane fields in Queensland, Australia. *GISci. Remote Sens.* 55 (2), 285–305. <http://dx.doi.org/10.1080/15481603.2017.1417691>.
- Johnson, B.A., Scheyvens, H., Shivakoti, B.R., 2014. An ensemble pansharpening approach for finer-scale mapping of sugarcane with landsat 8 imagery. *Int. J. Appl. Earth Obs. Geoinf.* 33, 218–225. <http://dx.doi.org/10.1016/j.jag.2014.06.003>, URL: <https://www.sciencedirect.com/science/article/pii/S0303243414001366>.
- Johnson, R.A., Wichern, D.W., 2014. *Applied Multivariate Statistical Analysis*, vol. 6, Pearson London, UK, http://dx.doi.org/10.1007/978-3-662-45171-7_14.
- Jordan, C.F., 1969a. Derivation of leaf-area index from quality of light on the forest floor. *Ecology* 50 (4), 663–666. <http://dx.doi.org/10.2307/1936256>.
- Jordan, C.F., 1969b. Derivation of leaf-area index from quality of light on the forest floor. *Ecology* 50 (4), 663–666. <http://dx.doi.org/10.2307/1936256>.
- Julien, M.H.R., Irvine, J.E., Benda, G.T.A., 1989. Sugarcane anatomy, morphology and physiology. In: *Diseases of Sugarcane*. Elsevier, Amsterdam, pp. 1–20. <http://dx.doi.org/10.1016/B978-0-444-42797-7.50005-3>.
- Karnieli, A., Agam, N., Pinker, R.T., Anderson, M., Imhoff, M.L., Gutman, G.G., Panov, N., Goldberg, A., 2010. Use of NDVI and land surface temperature for drought assessment: Merits and limitations. *J. Clim.* 23 (3), 618–633. <http://dx.doi.org/10.1175/2009JCLI2900.1>, URL: <https://journals.ametsoc.org/view/journals/clim/23/3/2009jcli2900.1.xml>.
- Kaufman, Y.J., Tanre, D., 1992. Atmospherically resistant vegetation index (ARVI) for EOS-MODIS. *IEEE Trans. Geosci. Remote Sens.* 30 (2), 261–270. <http://dx.doi.org/10.1109/36.134076>.
- Keith, J.C., 2002. Final Report - SRDC Project IPB001 Strategies to Control Greyback Canegrub in Early Harvested Ratoon Crops. Report, BSES, pp. 71–88.
- Koike, H., Gillaspie, A.G., 1989. CHAPTER XIX - mosaic. In: Ricard, C., Egan, B., Gillaspie, A., Hughes, C. (Eds.), *Diseases of Sugarcane*. Elsevier, Amsterdam, pp. 301–322. <http://dx.doi.org/10.1016/B978-0-444-42797-7.50023-5>.
- L3Harris Software & Technology Inc, 2022. ENVI. <https://www.l3harrisgeospatial.com/Software-Technology/ENVI>. (Accessed: 25/04/2022).
- Li, H., Yuan, X., Han, Y., Chen, J., Chen, X., 2019. Monitoring of sugarcane crop based on time series of sentinel-1 data. In: 2019 SAR in Big Data Era. BIGSARDATA, pp. 1–6. <http://dx.doi.org/10.1109/BIGSARDATA.2019.8858450>.
- Liang, S., Wang, J. (Eds.), 2020. Atmospheric correction of optical imagery. In: *Advanced Remote Sensing (Second Edition)*. Academic Press, pp. 131–156. <http://dx.doi.org/10.1016/B978-0-12-815826-5.00004-0>.
- Louhaichi, M., Borman, M.M., Johnson, D.E., 2001. Spatially located platform and aerial photography for documentation of grazing impacts on wheat. *Geocarto Int.* 16 (1), 65–70.
- Lu, G., Wang, Z., Xu, F., Pan, Y.B., Grisham, M.P., Xu, L., 2021. Sugarcane mosaic disease: Characteristics, identification and control. *Microorganisms* 9 (9), 1984.
- Macedo, N., Macedo, D., de Campos, M.B.S., Novaretti, W.R., Ferraz, L.C.C., 2015. Chapter 5 - management of pests and nematodes. In: Santos, F., Borém, A., Caldas, C. (Eds.), *Sugarcane*. Academic Press, San Diego, pp. 89–113. <http://dx.doi.org/10.1016/B978-0-12-802239-9.00005-0>.
- Magarey, R., 2021. Ratoon Stunting Disease. Report, SRA.
- Magarey, R., McHardie, R., Hession, M., Cripps, G., Burgess, D., Spannagle, B., Sutherland, P., Di Bella, L., Milla, R., Millar, F., Schembri, A., Baxter, D., Hetherington, M., Turner, M., Jakins, A., Quinn, B., Kalkhoran, S., Gibbs, L., Ngo, C., 2021. Incidence and economic effects of ratoon stunting disease on the Queensland sugarcane industry : ASSCT peer-reviewed paper. In: *Proceedings of the Australian Society of Sugar Cane Technologists*, vol. 42, pp. 520–526.
- Magarey, R., Neilsen, W., Bull, J., 2004. The effect of orange rust on sugarcane yield in breeding selection trials in central Queensland: 1999–2001. In: *2004 Conference of the Australian Society of Sugar Cane Technologists Held At Brisbane, Queensland, Australia*. 4-7 May 2004, pp. 1–6.
- Magarey, R., Neilsen, W., Bull, J., 2022. *Diseases of Australian Sugarcane Field Guide*. BSES.
- Matsuoka, S., Maccheroni, W., 2015. Chapter 6 - disease management. In: Santos, F., Borém, A., Caldas, C. (Eds.), *Sugarcane*. Academic Press, San Diego, pp. 115–132. <http://dx.doi.org/10.1016/B978-0-12-802239-9.00006-2>.
- McFeeters, S.K., 1996. The use of the normalized difference water index (NDWI) in the delineation of open water features. *Int. J. Remote Sens.* 17 (7), 1425–1432. <http://dx.doi.org/10.1080/01431169608948714>.
- McNairn, H., Shang, J., 2016. A review of multitemporal synthetic aperture radar (SAR) for crop monitoring. In: *Multitemporal Remote Sensing: Methods and Applications*. Springer, pp. 317–340.
- Merzlyak, M.N., Gitelson, A.A., Chivkunova, O.B., Rakitin, V.Y., 1999a. Non-destructive optical detection of pigment changes during leaf senescence and fruit ripening. *Physiol. Plant.* 106 (1), 135–141. <http://dx.doi.org/10.1034/j.1399-3054.1999.106119.x>.
- Merzlyak, M.N., Gitelson, A.A., Chivkunova, O.B., Rakitin, V.Y., 1999b. Non-destructive optical detection of pigment changes during leaf senescence and fruit ripening. *Physiol. Plant.* 106 (1), 135–141.
- Merzlyak, M.N., Gitelson, A.A., Chivkunova, O.B., Rakitin, V.Y., 1999c. Non-destructive optical detection of pigment changes during leaf senescence and fruit ripening. *Physiol. Plant.* 106 (1), 135–141. <http://dx.doi.org/10.1034/j.1399-3054.1999.106119.x>.
- Militante, S.V., Gerardo, B.D., Medina, R.P., 2019. Sugarcane disease recognition using deep learning. In: 2019 IEEE Eurasia Conference on IOT, Communication and Engineering. ECICE, pp. 575–578. <http://dx.doi.org/10.1109/ECICE47484.2019.8942690>.
- Moriya, E.A.S., Imai, N.N., Tommaselli, A.M.G., Miyoshi, G.T., 2017. Mapping mosaic virus in sugarcane based on hyperspectral images. *IEEE J. Sel. Top. Appl. Earth Obs. Remote Sens.* 10 (2), 740–748. <http://dx.doi.org/10.1109/JSTARS.2016.2635482>.

- Moriya, E.A.S., Tommaselli, A.M.G., Imai, N.N., 2018. A study on the effects of viewing angle variation in sugarcane radiometric measures. *Boletim Ciencias Geodesicas* 24 (1), 85–97. <http://dx.doi.org/10.1590/S1982-21702018000100007>.
- Narmilan, A., Gonzalez, F., Salgado, A.S.A., Powell, K., 2022. Detection of white leaf disease in sugarcane using machine learning techniques over UAV multispectral images. *Drones* 6 (9), 230. <http://dx.doi.org/10.3390/drones6090230>.
- NASA, 2022a. Landsat Missions, landsat 7. <https://www.usgs.gov/landsat-missions/landsat-7>. (Accessed 01 May 2022).
- NASA, 2022b. Landsat missions, landsat 8. <https://www.usgs.gov/landsat-missions/landsat-8>. (Accessed 01 May 2022).
- NASA, 2022c. Landsat missions, landsat 9. <https://www.usgs.gov/landsat-missions/landsat-9>. (Accessed 01 May 2022).
- Nikos Alexandratos, J.B., 2012. World agriculture towards 2030/2050: the 2012 revision. *ESA* 12–03, <http://dx.doi.org/10.22004/ag.econ.288998>.
- Ong, P., Jian, J., Li, X., Zou, C., Yin, J., Ma, G., 2023. New approach for sugarcane disease recognition through visible and near-infrared spectroscopy and a modified wavelength selection method using machine learning models. *Spectrochim. Acta Part A: Mol. Biomol. Spectrosc.* 302, 123037. <http://dx.doi.org/10.1016/j.saa.2023.123037>.
- Pandey, S., van Nistelrooij, M., Maasackers, J.D., Sutar, P., Houweling, S., Varon, D.J., Tol, P., Gains, D., Worden, J., Aben, I., 2023. Daily detection and quantification of methane leaks using sentinel-3: a tiered satellite observation approach with sentinel-2 and sentinel-5p. *Remote Sens. Environ.* 296, 113716. <http://dx.doi.org/10.1016/j.rse.2023.113716>.
- QGIS Development Team, 2024. QGIS Geographic Information System. QGIS Association, URL: <https://www.qgis.org>.
- Qi, J., Chehbouni, A., Huete, A., Kerr, Y., Sorooshian, S., 1994. A modified soil adjusted vegetation index. *Remote Sens. Environ.* 48 (2), 119–126. [http://dx.doi.org/10.1016/0034-4257\(94\)90134-1](http://dx.doi.org/10.1016/0034-4257(94)90134-1), URL: <https://www.sciencedirect.com/science/article/pii/0034425794901341>.
- Rahman, M.M., Robson, A.J., 2016. A novel approach for sugarcane yield prediction using landsat time series imagery: A case study on Bundaberg region. *Adv. Remote Sens.* 5 (2), 93–102.
- Ramouthar, P., McFarlane, S., Berry, S., Rutherford, R., 2013. Yield loss due to sugarcane yellow leaf virus and its prevalence in the South African sugar industry. In: *South African Sugar Technologists' Association*. pp. 244–254.
- Rassaby, L., Girard, J.C., Letourmy, P., Chaume, J., Irely, M., Lockhart, B., Kodja, H., Rott, P., 2003. Impact of sugarcane yellow leaf virus on sugarcane yield and juice quality in Réunion island. *Eur. J. Plant Pathol.* 109, 459–466. <http://dx.doi.org/10.1023/A:1024211823306>.
- Ratnasari, E.K., Mentari, M., Dewi, R.K., Hari Ginardi, R.V., 2014. Sugarcane leaf disease detection and severity estimation based on segmented spots image. In: *Proceedings of International Conference on Information, Communication Technology and System. (ICTS) 2014*, pp. 93–98. <http://dx.doi.org/10.1109/ICTS.2014.7010564>.
- ReSe, 2022. ReSe - remote sensing applications. URL: <https://www.rese-apps.com/index.html>.
- Rondeaux, G., Steven, M., Baret, F., 1996. Optimization of soil-adjusted vegetation indices. *Remote Sens. Environ.* 55 (2), 95–107. [http://dx.doi.org/10.1016/0034-4257\(95\)00186-7](http://dx.doi.org/10.1016/0034-4257(95)00186-7), URL: <https://www.sciencedirect.com/science/article/pii/0034425795001867>.
- Rouse, J.W., Haas, R.H., Schell, J.A., Deering, D.W., et al., 1974. Monitoring vegetation systems in the great plains with ERTS. *NASA Spec. Publ.* 351 (1), 309.
- Roy, P.S., 1989. Spectral reflectance characteristics of vegetation and their use in estimating productive potential. *Proceedings: Plant Sci.* 99, 59–81.
- Roy, P.S., Ravan, S.A., 1996. Biomass estimation using satellite remote sensing data—An investigation on possible approaches for natural forest. *J. Biosci.* 21 (4), 535–561. <http://dx.doi.org/10.1007/BF02703218>.
- Sahoo, R., Ray, S., R. M., 2015. Hyperspectral remote sensing of agriculture. *Curr. Sci.* 108, 848–859.
- Sallam, N., 2011. Review of current knowledge on the population dynamics of dermolepida albhirtum (Waterhouse) (Coleoptera: Scarabaeidae). *Aust. J. Entomol.* 50 (3), 300–308. <http://dx.doi.org/10.1111/j.1440-6055.2010.00807.x>.
- Sanches, G.M., Duft, D.G., Kölln, O.T., dos Santos Luciano, A.C., Castro, S.G.Q.D., Okuno, F.M., Franco, H.C.J., 2018. The potential for RGB images obtained using unmanned aerial vehicle to assess and predict yield in sugarcane fields. *Int. J. Remote Sens.* 39 (15–16), 5402–5414. <http://dx.doi.org/10.1080/01431161.2018.1448484>.
- Sara, D., Mandava, A.K., Kumar, A., Duela, S., Jude, A., 2021a. Hyperspectral and multispectral image fusion techniques for high resolution applications: A review. *Earth Sci. Inform.* 14 (4), 1685–1705.
- Sara, D., Mandava, A.K., Kumar, A., Duela, S., Jude, A., 2021b. Hyperspectral and multispectral image fusion techniques for high resolution applications: a review. *Earth Sci. Inform.* 14, 1685–1705. <http://dx.doi.org/10.1007/s12145-021-00621-6>.
- Shendryk, Y., Sofonia, J., Garrard, R., Rist, Y., Skocaj, D., Thorburn, P., 2020. Fine-scale prediction of biomass and leaf nitrogen content in sugarcane using UAV LiDAR and multispectral imaging. *Int. J. Appl. Earth Obs. Geoinf.* 92, 102177.
- SIIS, 2010. KOMPSAT series. <http://www.si-imaging.com/products>. (Accessed 30 September 2010).
- Simões, I.O., Rios do Amaral, L., 2023. UAV-based multispectral data for sugarcane resistance phenotyping of orange and brown rust. *Smart Agric. Technol.* 4, 100144. <http://dx.doi.org/10.1016/j.atech.2022.100144>.
- Sims, D.A., Gamon, J.A., 2002. Relationships between leaf pigment content and spectral reflectance across a wide range of species, leaf structures and developmental stages. *Remote Sens. Environ.* 81 (2), 337–354. [http://dx.doi.org/10.1016/S0034-4257\(02\)00010-X](http://dx.doi.org/10.1016/S0034-4257(02)00010-X), URL: <https://www.sciencedirect.com/science/article/pii/S003442570200010X>.
- Singh, S., Rao, G., Singh, J., Singh, S., 1997. Effect of sugarcane mosaic potyvirus infection on metabolic activity, yield and juice quality. *Sugar Cane (United Kingdom)*.
- Singh, M., Singh, A., Upadhyaya, P., Rao, G., 2005. Transmission studies on an Indian isolate of sugarcane mosaic potyvirus. *Sugar Tech* 7 (2), 32–38.
- Singh, V., Sinha, O., Kumar, R., 2003. Progressive decline in yield and quality of sugarcane due to sugarcane mosaic virus. *Indian Phytopath.* 56, 500–502.
- Slagter, B., Reiche, J., Marcos, D., Mullissa, A., Lossou, E., Peña-Claros, M., Herold, M., 2023. Monitoring direct drivers of small-scale tropical forest disturbance in near real-time with sentinel-1 and -2 data. *Remote Sens. Environ.* 295, 113655. <http://dx.doi.org/10.1016/j.rse.2023.113655>.
- Soca-Muñoz, J.L., Rodríguez-Machado, E., Aday-Díaz, O., Hernández-Santana, L., Orozco-Morales, R., 2020. Spectral signature of brown rust and orange rust in sugarcane. *Rev. Fac. Ing. Univ. Antioquia* 9–20. <http://dx.doi.org/10.17533/udea.redin.20191042>.
- Som-ard, J., Atzberger, C., Izquierdo-Verdiguier, E., Vuolo, F., Immitzer, M., 2021. Remote sensing applications in sugarcane cultivation: A review. *Remote Sens.* 13 (20), 4040. <http://dx.doi.org/10.3390/rs13204040>.
- SRA, 2022. Variety Guide 2022/2023 Herbert Region. Report, SRA.
- Srivastava, S., Kumar, P., Mohd, N., Singh, A., Gill, F.S., 2020. A novel deep learning framework approach for sugarcane disease detection. *SN Comput. Sci.* 1, 1–7.
- Storch, T., 2022. Earth observation center, EnMAP. https://www.dlr.de/eoc/en/desktopdefault.aspx/tabid-5514/20470_read-47899/. (Accessed 01 May 2022).
- Sudianto, S., Herdiyeni, Y., Prasetyo, L.B., 2023. Classification of sugarcane area using landsat 8 and random forest based on phenology knowledge. *JOIV: Int. J. Inform. Vis.* 7 (3–2), 1974–1981.
- Susantoro, T.M., Wikantika, K., Harto, A.B., Suwardi, D., 2019. Monitoring sugarcane growth phases based on satellite image analysis (A case study in indramayu and its surrounding, west Java, Indonesia). *HAYATI J. Biosci.* 26 (3), 117. <http://dx.doi.org/10.4308/hjb.26.3.117>.
- Tilman, D., Balzer, C., Hill, J., Befort, B.L., 2011. Global food demand and the sustainable intensification of agriculture. In: *Proceedings of the National Academy of Sciences*, vol. 108, (50), pp. 20260–20264. <http://dx.doi.org/10.1073/pnas.1116437108>.
- Tucker, C.J., 1979. Red and photographic infrared linear combinations for monitoring vegetation. *Remote Sens. Environ.* 8 (2), 127–150. [http://dx.doi.org/10.1016/0034-4257\(79\)90013-0](http://dx.doi.org/10.1016/0034-4257(79)90013-0).
- Vargas, L.A.O., Mendoza, G.G., Gómez, R.A., Rivero, N.A., Espinosa, L.Y., 2016. Characterization of diatraea saccharalis in sugarcane (saccharum officinarum) with field spectroradiometry. *Int. J. Environ. Agric. Res. (IJOEAR)*.
- Vincini, M., Frazzi, E., 2011. Comparing narrow and broad-band vegetation indices to estimate leaf chlorophyll content in planophile crop canopies. *Precis. Agric.* 12, 334–344. <http://dx.doi.org/10.1007/s11119-010-9204-3>.
- Walthall, C.L., Norman, J.M., Welles, J.M., Campbell, G., Blad, B.L., 1985. Simple equation to approximate the bidirectional reflectance from vegetative canopies and bare soil surfaces. *Appl. Opt.* 24 (3), 383–387. <http://dx.doi.org/10.1364/AO.24.000383>.
- Wang, X.Y., Cang, X.Y., Qin, W., Shan, H.L., Zhang, R.Y., Wang, C.M., Li, W.F., Huang, Y.K., 2021. Evaluation of field resistance to brown stripe disease in novel and major cultivated sugarcane varieties in China. *J. Plant Pathol.* 103 (3), 985–989. <http://dx.doi.org/10.1007/s42161-021-00870-w>.
- Wang, J., Xiao, X., Liu, L., Wu, X., Qin, Y., Steiner, J.L., Dong, J., 2020. Mapping sugarcane plantation dynamics in Guangxi, China, by time series sentinel-1, sentinel-2 and landsat images. *Remote Sens. Environ.* 247, 111951. <http://dx.doi.org/10.1016/j.rse.2020.111951>, URL: <https://www.sciencedirect.com/science/article/pii/S0034425720303217>.
- Way, M., Leslie, G., Keeping, M., Govender, A., et al., 2006. Incidence of fulmekiola serrata (thysanoptera: Thripidae) in south african sugarcane. In: *Proceedings of the South African Sugar Technologists' Association*, vol. 80, pp. 199–201.
- Way, M., Rutherford, R., Sewpersad, C., Leslie, G., Keeping, M., 2010. Impact of sugarcane thrips, fulmekiola serrata (kobus) (thysanoptera: Thripidae) on sugarcane yield in field trials. In: *Proceedings of the South African Sugar Technologists' Association*, vol. 83, pp. 244–256.
- Xu, Y., Li, X., Du, H., Mao, F., Zhou, G., Huang, Z., Fan, W., Chen, Q., Ni, C., Guo, K., 2023. Improving extraction phenology accuracy using SIF coupled with the vegetation index and mapping the spatiotemporal pattern of bamboo forest phenology. *Remote Sens. Environ.* 297, 113785. <http://dx.doi.org/10.1016/j.rse.2023.113785>.
- Xue, J., Su, B., 2017. Significant remote sensing vegetation indices: A review of developments and applications. *J. Sens.* 2017, 1353691. <http://dx.doi.org/10.1155/2017/1353691>.
- Yamane, T., 2019. Sugarcane.

- Yilmaz, V., Gungor, O., 2016. Fusion of very high-resolution UAV images with criteria-based image fusion algorithm. *Arab. J. Geosci.* 9, 1–16.
- Young, A.J., Kawamata, A., Ensby, M.A., Lambley, E., Nock, C.J., 2016. Efficient diagnosis of ratoon stunting disease of sugarcane by quantitative PCR on pooled leaf sheath biopsies. *Plant Dis.* 100 (12), 2492–2498. <http://dx.doi.org/10.1094/PDIS-06-16-0848-RE>, PMID: 30686165.
- Zabel, F., Putzenlechner, B., Mauser, W., 2014. Global agricultural land resources—a high resolution suitability evaluation and its perspectives until 2100 under climate change conditions. *PLoS One* 9 (9), e107522. <http://dx.doi.org/10.1371/journal.pone.0107522>.
- Zarco-Tejada, P., Berjón, A., López-Lozano, R., Miller, J., Martín, P., Cachorro, V., González, M., de Frutos, A., 2005. Assessing vineyard condition with hyperspectral indices: Leaf and canopy reflectance simulation in a row-structured discontinuous canopy. *Remote Sens. Environ.* 99 (3), 271–287. <http://dx.doi.org/10.1016/j.rse.2005.09.002>.
- Zhu, Y.J., Lim, S.T.S., Schenck, S., Arcinas, A., Komor, E., 2010. RT-PCR and quantitative real-time RT-PCR detection of sugarcane yellow leaf virus (SCYLV) in symptomatic and asymptomatic plants of hawaiian sugarcane cultivars and the correlation of SCYLV titre to yield. *Eur. J. Plant Pathol.* 127 (2), 263–273. <http://dx.doi.org/10.1007/s10658-010-9591-3>.